



**HAL**  
open science

## The human remains from Axlor (Dima, Biscay, Northern Iberian Peninsula)

Asier Gómez-Olivencia, Diego López-Onaindia, Nohemi Sala, Antoine Balzeau, Ana Pantoja-Pérez, Ignacio Arganda-Carreras, Mikel Arlegi, Joseba Rios-Garaizar, Aida Gómez-Robles

► **To cite this version:**

Asier Gómez-Olivencia, Diego López-Onaindia, Nohemi Sala, Antoine Balzeau, Ana Pantoja-Pérez, et al.. The human remains from Axlor (Dima, Biscay, Northern Iberian Peninsula). *American Journal of Physical Anthropology*, 2020, 172 (3), pp.475-491. 10.1002/ajpa.23989 . hal-03006439

**HAL Id: hal-03006439**

**<https://hal.science/hal-03006439>**

Submitted on 15 Nov 2020

**HAL** is a multi-disciplinary open access archive for the deposit and dissemination of scientific research documents, whether they are published or not. The documents may come from teaching and research institutions in France or abroad, or from public or private research centers.

L'archive ouverte pluridisciplinaire **HAL**, est destinée au dépôt et à la diffusion de documents scientifiques de niveau recherche, publiés ou non, émanant des établissements d'enseignement et de recherche français ou étrangers, des laboratoires publics ou privés.



Distributed under a Creative Commons Attribution - NonCommercial - ShareAlike 4.0 International License



**The human remains from Axlor (Dima, Biscay, Northern Iberian Peninsula)**

Journal:	<i>American Journal of Physical Anthropology</i>
Manuscript ID	AJPA-2019-00291.R1
Wiley - Manuscript type:	Research Article
Date Submitted by the Author:	n/a
Complete List of Authors:	Gómez-Olivencia, Asier; Universidad del Pais Vasco, Departamento de Estratigrafía y Paleontología; López-Onaindia, Diego; Autonomous University of Barcelona (UAB), Biología Animal, Biología Vegetal i d'Ecologia Sala, Nohemi; Centro UCM-ISCIIE de Investigación sobre la Evolución y Comportamiento Humanos Balzeau, A; Museum Natl Hist Nat, Dept Prehist, CNRS UMR 7194 du CNRS, Paris, France , Dept. of Prehistory Pantoja-Pérez, Ana; Centro UCM-ISCIIE de Investigación sobre la Evolución y Comportamiento Humanos Arganda-Carreras, Ignacio; Dept. Ciencias de la Computacion e Inteligencia Artificial. Facultad de Informatica, Universidad del País Vasco-Euskal Herriko Unibertsitatea (UPV/EHU) Manuel Lardizabal Ibilbidea 1, 20018 Donostia, Gipuzkoa, Spain. Arlegi, Mikel; Universidad del Pais Vasco, Estatigrafía y Paleontología Rios-Garaizar, Joseba; CENIEH Gómez-Robles, Aida; Konrad Lorenz Institute for Evolution and Cognition Research
Key Words:	Neandertal, anatomically modern humans, enamel-dentine junction, geometric morphometrics, Paleolithic
Subfield: Please select 2 subfields. Select the main subject first.:	Paleontology , Human biology [living humans; behavior, ecology, physiology, anatomy]

SCHOLARONE™  
Manuscripts

The human remains from Axlor (Dima, Biscay, Northern Iberian Peninsula)

Asier Gómez-Olivencia<sup>a,b,c,d\*</sup>

Diego López-Onaindia<sup>eOnaindiad</sup>

Nohemi Sala<sup>f,dSalae,e</sup>

Antoine Balzeau<sup>g,hBalzeauf,g</sup>

Ana Pantoja-Pérez<sup>dPantojae</sup>

Ignacio Arganda-Carreras<sup>i,jCarrerash,b,i</sup>

Mikel Arlegi<sup>a,kj</sup>

Joseba Rios-Garaizar<sup>fGaraizare</sup>

Aida Gómez-Robles<sup>l,m,nRoblesk,l,m</sup>

<sup>a</sup>Dept. Estratigrafía y Paleontología, Facultad de Ciencia y Tecnología, Universidad del País Vasco-Euskal Herriko Unibertsitatea (UPV/EHU). Barrio Sarriena s/n, 48940 Bilbao, Spain.

<sup>b</sup>IKERBASQUE. Basque Foundation for Science, [Bilbao, Spain](#).

<sup>c</sup>[Sociedad de Ciencias Aranzadi, Zorroagaina 11, 20014 Donostia-San Sebastian, Spain.](#)

<sup>d</sup>~~Centro~~<sup>e</sup>Centro UCM-ISCIH de Investigación sobre Evolución y Comportamiento Humanos, Avda. Monforte de Lemos 5 (Pabellón 14), 28029 Madrid, Spain.

<sup>e</sup>~~GREAB~~<sup>d</sup>GREAB, Unitat d'Antropologia Biològica, Departament de Biologia Animal, Biologia Vegetal i Ecologia, Facutat de Biociències, Universitat Autònoma de Barcelona, 08193 Bellaterra, Spain.

<sup>f</sup>~~Centro~~<sup>e</sup>Centro Nacional de Investigación sobre la Evolución Humana (CENIEH), Paseo de la Sierra de Atapuerca 3, 09002 Burgos, Spain.

<sup>g</sup><sup>f</sup>Équipe de Paléontologie Humaine, UMR 7194, CNRS, Département Homme et Environnement, Muséum national d'Histoire naturelle. Musée de l'Homme, 17, Place du Trocadéro, 75016 Paris, France

<sup>h</sup>Department<sup>g</sup>~~Department~~ of African Zoology, Royal Museum for Central Africa, Tervuren, Belgium

<sup>i</sup>Dept<sup>h</sup>~~Dept~~. Ciencias de la Computacion e Inteligencia Artificial. Facultad de Informatica, Universidad del País Vasco-Euskal Herriko Unibertsitatea (UPV/EHU) Manuel Lardizabal Ibilbidea 1, 20018 Donostia, Gipuzkoa, Spain.

<sup>j</sup>Donostia<sup>i</sup>~~Donostia~~ International Physics Center (DIPC). Manuel Lardizabal Ibilbidea 4, 20018 Donostia, Gipuzkoa, Spain.

<sup>k</sup>Universit<sup>i</sup>~~Université~~ de Bordeaux, PACEA UMR 5199, Bâtiment B8, Allée Geoffroy Saint-Hilaire, 33615 Pessac, France.

<sup>l</sup>Department<sup>k</sup>~~Department~~ of Anthropology, University College London, WC1E 0BW London, UK.

<sup>m</sup>Department<sup>l</sup>~~Department~~ of Genetics, Evolution and Environment, University College London, WC1E 6BT London, UK.

<sup>n</sup>Department<sup>m</sup>~~Department~~ of Life Sciences, Natural History Museum, SW7 5BD London, UK.

#### Correspondence

Asier Gómez-Olivencia, Dept. Estratigrafía y Paleontología, Facultad de Ciencia y Tecnología, Universidad del País Vasco-Euskal Herriko Unibertsitatea (UPV/EHU). Barrio Sarriena s/n, 48940 Bilbao, Spain.

Email: asier.gomez@ehu.eus (A.G.-O.)

## Abstract

**Objectives:** We provide the description and comparative analysis of all the human fossil remains found at Axlor during the excavations carried out by J.M. Barandiarán from 1967 to 1974: a cranial vault fragment and eight teeth, five of which likely belonged to the same individual, although two are currently lost. Our goal is to describe in detail all these human remains and discuss both their taxonomic attribution and their stratigraphic context.

**Materials and methods:** We describe external and internal anatomy, and use classic and geometric morphometrics. The teeth from Axlor are compared to Neandertals, Upper Paleolithic and recent modern humans.

**Results:** Three teeth (a left  $dm^2$ , a left  $di^1$ , and a right  $I_1$ ) and the parietal fragment show morphological features consistent with a Neanderthal classification, and were found in an undisturbed Mousterian context. The remaining three teeth (plus the two lost ones), initially classified as Neandertals, show morphological features and a general size that are more compatible with their classification as modern humans.

**Discussion:** The combined anatomical and stratigraphic study suggest that the remains of two different adult Neandertals have been recovered during the old excavations performed by Barandiarán: a left parietal fragment (level VIII) and a right  $I_1$  (level V). Additionally, two different Neanderthal children lost deciduous teeth during the formations of levels V (left  $di^1$ ) and IV (right  $dm^2$ ). In addition, a modern human individual is represented by five remains (two currently lost) from a complex stratigraphic setting. Some of the morphological features of these remains suggest that they may represent one of the scarce examples of Upper Paleolithic modern human remains in the northern Iberian Peninsula, which should be confirmed by further testing.

1  
2  
3  
4  
5  
6  
7  
8  
9  
10  
11  
12  
13  
14  
15  
16  
17  
18  
19  
20  
21  
22  
23  
24  
25  
26  
27  
28  
29  
30  
31  
32  
33  
34  
35  
36  
37  
38  
39  
40  
41  
42  
43  
44  
45  
46  
47  
48  
49  
50  
51  
52  
53  
54  
55  
56  
57  
58  
59  
60

**KEYWORDS**

Neandertal, anatomically modern humans, enamel-dentine junction, geometric morphometrics,  
Paleolithic

## 1-Introduction

The rock-shelter of Axlor is located in the mountainous region included in the national park of Urkiola (Biscay, Basque Country) and preserves one of the most important Middle Paleolithic sequences in the northern Iberian Peninsula (Figure 1). Axlor was discovered in 1932 by the Basque prehistorian J. M. Barandiarán. The first archaeological excavations took place in 1967, and encompassed a total of eight field seasons until 1974 (Barandiarán, 1980). These excavations revealed a sequence of nine layers (I-IX), in which Middle Paleolithic lithic assemblages were found in levels III to VIII. Recent excavations (2000-2008) directed by González-Urquijo, Ibáñez and Rios-Garaizar, provide a new stratigraphic sequence, roughly equivalent to the previous one, but with additional levels, not previously identified or excavated by Barandiarán. Some of these levels were deposited before level VIII, but their chronology remains uncertain (González-Urquijo, Ibáñez, Lazuén & Mozota, 2014; Rios-Garaizar, 2017). Additionally, an early Upper Paleolithic occupation has been recognized (level A of the new excavations, equivalent to the base of Barandiarán's level II, previously considered sterile; González-Urquijo et al., 2014). Ultra-filtered dates obtained from red deer with anthropogenic marks from level IV have yielded results that go beyond the radiocarbon limit, correcting previous dating which situated this level at the very end of regional Middle Paleolithic (Marín-Arroyo et al., 2018). Across the sequence, there are clear differences in terms of the technological characteristics, percentage of ungulate taxa consumed, and type of occupation of the cave between the upper (III-VI) and lower levels (VII-VIII) of the Mousterian sequence, which has been confirmed during the recent excavations (Altuna, 1989; Castaños, 2005; González-Urquijo et al., 2014; Rios-Garaizar, 2017). Recent reassessment of the Barandiarán collection has identified the presence of bird and carnivore exploitation for the first time during the Middle Paleolithic of the Cantabrian region: at least a golden eagle and a lynx where exploited for dietary purposes (Gómez-Olivencia et al., 2018a).

1  
2 [INSERT FIGURE 1 HERE]  
3  
4  
5

6 The current human fossil record published for Axlor is limited to five upper left dental  
7 remains (C, P<sup>4</sup>-M<sup>3</sup>) with a maxilla fragment, likely belonging to the same individual (a young  
8 adult), which were found in 1967 from a level with Quina Mousterian lithics and faunal remains of  
9 red deer, reindeer, and steppe bison (Basabe, 1973; [Figure 2](#)). Basabe (1973) seems to be cautious  
10 in the taxonomic assessment of these remains. While he considers that the morphology of these  
11 dental remains is compatible with that found in similar (Mousterian) archaeological contexts, he  
12 nonetheless considers these remains as “evolved”, with “intermediate” size and traits, including the  
13 “unclear” taurodontism in M1-M2 (Basabe, 1973). Currently, only three (P<sup>4</sup>, M<sup>1</sup>, M<sup>3</sup>) of these  
14 remains are curated at the Arkeologi Museoa (Bilbao), whereas the location of the other teeth is  
15 unknown. A more recent reassessment of these teeth supported a Neandertal classification based on  
16 their size and the alleged presence of taurodontism in the molars (Rostro-Carmona, 2013).  
17 However, a visual inspection of the morphology of the M<sup>1</sup> shows that it does not present the typical  
18 Neandertal morphology for this tooth (e.g., Bailey, 2004; Gómez-Robles et al., 2007). Moreover, no  
19 study of the internal anatomy of the teeth based on virtual anthropology techniques has been  
20 performed, which could provide a more accurate taxonomic assessment. In 2005, the re-assessment  
21 of the whole Barandiarán collection (coordinated by J.E. González Urquijo) resulted in the  
22 recognition of three additional human remains: two teeth and a cranial fragment. More recently, the  
23 reassessment of the faunal collection from Barandiarán's excavation has resulted in the  
24 identification of an additional human remain among the faunal remains: an upper deciduous molar.  
25  
26  
27  
28  
29  
30  
31  
32  
33  
34  
35  
36  
37  
38  
39  
40  
41  
42  
43  
44  
45  
46  
47  
48  
49  
50  
51

52 [INSERT FIGURE 2 HERE]  
53  
54  
55  
56

57 Here we provide a detailed description and comparative analysis of all the human fossil  
58 remains from Axlor found during J.M. Barandiarán's excavations, including a taphonomic analysis  
59  
60



1  
2 of the cranial fragment. This study also reassess the taxonomic affinities of the remains published  
3  
4 by Basabe (1973) and Rostro-Carmona (2013), and discusses the archaeological context of all the  
5  
6 human remains from this collection. In fact, the revision of the archaeological context from the  
7  
8 field-notes taken by J.M. de Barandiarán at the site casts doubts on the stratigraphic position of all  
9  
10 the teeth studied by Basabe (1973) and Rostro-Carmona (2013), while in the rest of the cases the  
11  
12 association of these human remains to Mousterian contexts seems secure ([Supplementary](#)  
13  
14 [Information Text S1](#)).  
15  
16  
17  
18  
19  
20  
21  
22

## 23 **2-Materials and Methods**

### 24 *2.1-Materials*

25  
26  
27  
28  
29  
30  
31  
32  
33  
34  
35  
36  
37  
38  
39  
40  
41  
42  
43  
44  
45  
46  
47  
48  
49  
50  
51  
52  
53  
54  
55  
56  
57  
58  
59  
60

The current collection of human remains from the Barandiarán excavations includes an upper fourth premolar, an upper first molar and an upper third molar from the same (young adult) individual (Basabe, 1973), a cranial fragment, a lower right central incisor, an upper left first deciduous incisor and a left upper deciduous second molar ([Table 1](#)). Their spatial location, according to the available information is shown in [Figure 2](#). Access to these materials was granted by the Arkeologi Museoa (Bilbao). The CT scans of these fossils, ~~and~~ the derived segmentation files, and 3D volumes are [freely accessible](#)~~accessible via XXX~~.

~~[Note to the Editor and the reviewers: All the original micro-CTs and the derived segmentation files and 3D volumes will be made accessible in a public repository (e.g., morphosource or figshare) and the corresponding DOIs will be included in the next version of this manuscript.]~~

[INSERT TABLE 1 HERE]

## 2.2-Micro-CT scanning

All the Axlor human remains were micro-CT scanned at the Spanish National Research Center for Human Evolution (CENIEH) using a Phoenix v/tome/x s (GE Measurement & Control). The resolution was maximized depending on the size of the different fossil remains (teeth: 18.99 $\mu$ m; cranial fragment: 33 $\mu$ m).

## 2.3-Anatomical descriptions

Standard methods were used to describe and analyze the external and internal anatomy of the cranial fragment. Previous knowledge of the anatomy and relative variation of exo and endocranial surfaces was used to identify the anatomical position and diagnostic features of the cranial fragment (e.g., Balzeau, 2013; Balzeau, Grimaud-Hervé & Gilissen, 2011; Balzeau et al., 2017). The teeth were described following ~~established~~ anatomical dental terms (Carlsen, 1987). In addition, we scored several non-metric traits following both the Arizona State University Dental Anthropology System (ASUDAS) (Turner, Nichol & Scott, 1991) and some complementary traits described by Bailey (2002), which were compared to Neandertals, Upper Paleolithic modern humans (UPMH) and recent humans (Martínón-Torres, Bermúdez de Castro, Gómez-Robles, Prado-Simón, & Arsuaga, 2012). Some of these traits were also scored in the EDJ surface and completed by the traits described by Martin, Hublin, Gunz, & Skinner (2017) for the molars. The roots of the incisors were measured following the method described by Le Cabec, Gunz, Kupczik, Braga & Hublin (2013): Root Length (RL), Root Volume (RV), Root Pulp Volume (RPV), Crown Pulp Volume (CrPV) and different ratios between these measurements. Dental wear assessment was based on Molnar (1971).

## 2.4-Bone thickness mapping (cranial fragment) and volume segmentation (teeth)

1  
2 The 3D variation of the total bone thickness of the cranial fragment was evaluated using the  
3  
4  
5  
6  
7  
8  
9  
10  
11  
12  
13  
14  
15  
16  
17  
18  
19  
20  
21  
22  
23  
24  
25  
26  
27  
28  
29  
30  
31  
32  
33  
34  
35  
36  
37  
38  
39  
40  
41  
42  
43  
44  
45  
46  
47  
48  
49  
50  
51  
52  
53  
54  
55  
56  
57  
58  
59  
60

The 3D variation of the total bone thickness of the cranial fragment was evaluated using the  
exo- and endocranial surfaces using the module Surface-Distance of Avizo 7. The results of this  
analysis were illustrated using a chromatic scale and compared to previous studies (Balzeau, 2013)  
in order to gain insights on the potential taxonomic significance of the thickness distribution  
pattern.

In the case of the teeth, before their segmentation, the CT image volumes were pre-  
processed using Fiji (Schindelin et al., 2012) by first converting them to 8-bit and then re-sampling  
them in the Z direction by a factor of 2 (final volume resolution: 0.019 x 0.019 x 0.038 microns per  
voxel). Next, the volumes were segmented using an interactive learning approach (Arganda-  
Carreras et al., 2017) that classified each voxel as belonging to one of the following classes: bone,  
dentine, enamel, or background. The pulp chamber was afterwards labeled by semi-automatic  
filling of the cavity inside the other teeth labels. The output label images were cleaned up by  
removing small artifacts and noise by means of morphological operations (Legland, Arganda-  
Carreras & Andrey, 2016). Finally, we performed manual correction of the segmented images using  
AvizoLite software due to the presence of cracks in some teeth, and lower density zones in the  
enamel some of the teeth.

### *2.5-Taphonomic analysis*

The cranial bone was macroscopically and microscopically examined using a hand lens and a  
stereoscopic zoom microscope (Olympus SZX10) to examine surface modifications. For the  
analysis of striae regarding the differentiation between cut marks and trampling marks we have used  
the protocol proposed by Domínguez-Rodrigo, de Juana, Galán & Rodríguez (2009). The cranial  
breakage pattern was analyzed following the criteria developed by Sala, Pantoja-Pérez, Arsuaga,  
Pablos & Martínez (2016) to assess the presence/absence of perimortem (fresh bone) and  
postmortem (dry bone) fractures. Four parameters were recorded: fracture outline (linear, depressed,

1  
2 stellate); fracture angle (right or oblique); fracture edge (smooth or jagged); presence/absence of  
3  
4 cortical delamination.  
5  
6  
7

## 8 9 *2.6-Geometric morphometrics*

10  
11 Geometric morphometric analyses of the occlusal surface of the premolar and molar crowns  
12  
13 were used to compare the Axlor posterior permanent teeth with the Neandertal and modern human  
14  
15 samples used in Gomez-Robles et al. (2007), Gómez-Robles, Bermúdez de Castro, Martínón-  
16  
17 Torres, Prado-Simón, & Arsuaga (2012), and Gómez-Robles, Martínón-Torres, Bermúdez de  
18  
19 Castro, Prado-Simón, & Arsuaga (2011). Modern human samples included both fossil and recent  
20  
21 modern humans. Occlusal photographs were used to place 2D configurations of landmarks and  
22  
23 semilandmarks. For the M<sup>1</sup>, analyses were repeated on the original photographs and on an occlusal  
24  
25 projection of the occlusal surface obtained after virtually correcting enamel cracks. Because the  
26  
27 Axlor M<sup>1</sup> is heavily worn, the location of anatomical landmarks on cusp apices cannot be  
28  
29 unequivocally determined. Therefore, M<sup>1</sup> analyses were repeated twice, using the original  
30  
31 configuration of landmarks and semilandmarks as described in Gómez-Robles et al. (2007) and only  
32  
33 the configuration of outline semilandmarks (after removing the four anatomical landmarks). The  
34  
35 second analysis, therefore, focuses on the ability of the M<sup>1</sup> occlusal outline to differentiate  
36  
37 Neandertal from modern human molars. The Axlor P<sup>4</sup> and M<sup>3</sup> are substantially less worn than the  
38  
39 M<sup>1</sup>, so only the complete configuration of landmarks and semilandmarks was evaluated for them.  
40  
41 For all the posterior teeth, geometric morphometric analyses were performed that included and  
42  
43 excluded size variation (in form and shape space, respectively). A discriminant analysis based on  
44  
45 the first ten principal components of shape variation was carried out to evaluate the species that  
46  
47 Axlor teeth are assigned to.  
48  
49  
50  
51  
52  
53  
54  
55  
56  
57  
58  
59  
60

## **3-Metric, morphological and taphonomic description**

1  
2  
3  
4 The cranial and the dental remains are described here. The comparison of the external crown  
5  
6 metric data between Axlor teeth and different comparative samples are shown in [Table 2](#). Only  
7  
8 taxonomically useful metric traits are discussed below.  
9  
10

11  
12  
13 [INSERT TABLE 2 HERE]  
14  
15  
16  
17

### 18 *3.1-Cranial ~~fragment~~remain*

19  
20 AX.11B.415.400 is a fragment (56 × 41 mm) of a left parietal bone, which preserves 54 mm  
21  
22 of the sagittal suture ([Figure 3](#)). The suture is not fused, and this left fragment has been separated  
23  
24 from the right parietal bone without any breakage of the indentations. Bone thickness for the  
25  
26 analyzed area is only slightly smaller than in La Ferrassie 1 (Balzeau, 2013) and thus incompatible  
27  
28 with a young immature status. Thus, the fragment is not from a child, but may belong to a young  
29  
30 adult or adult. The antero-posterior curvature of this fragment is not very pronounced.  
31  
32  
33  
34  
35

36 [INSERT FIGURE 3 HERE]  
37  
38  
39  
40

41 Bone thickness distribution was quantified on nearly the whole preserved area of this  
42  
43 fragment. Thickness varies between 3.4 mm and 10.5 mm. ~~The mean~~Mean thickness of the  
44  
45 fragment is 5.4 mm. Thickness is evenly distributed along the surface of the fragment, there is no  
46  
47 clear increase or decrease related to bone thickness variation. The only exception concerns the  
48  
49 blood vessels on the endocranial surface of the anterior border of the fragment, which are associated  
50  
51 with a clear thinning of the bone (the area with white dots at the anterior border of the bone, noted  
52  
53 V on [Figure 3](#)). Moreover, the infero-anterior corner of the fragment shows a slight increase in bone  
54  
55 thickness (represented by the purple area, noted PC on [Figure 3](#)) which continues posteriorly and  
56  
57 obliquely. It corresponds to the postcentral sulcus.  
58  
59  
60

1  
2  
3  
4 Some clear endocranial features are visible. Some branches of the meningeal system are  
5  
6 noticeable. They probably all belong to the anterior ramus, one being the anterior branch (noted A  
7  
8 on [Figure 3](#)), the second corresponding to the obelic branch (noted O on Fig. 3). The anterior branch  
9  
10 splits in two simple veins that are quite large. The obelic branch splits into two smaller and long  
11  
12 veins. Concerning the gyral pattern visible on this endocranial surface, two sulci are clear. The  
13  
14 course of the postcentral sulcus (noted PC on [Figure 3](#)) goes from the antero-inferior corner of the  
15  
16 fragment to the center of the medial border of the fragment. This sulcus is well printed and shows a  
17  
18 clear course. Anteriorly, the central sulcus (noted C on [Figure 3](#)) seems to run along the course of  
19  
20 the most anterior vein of the anterior ramus. Those two sulci have a parallel course, delimiting a  
21  
22 post-central gyrus that has a regular width on its preserved extension.  
23  
24  
25  
26  
27  
28

29  
30 Both bone thickness distribution pattern and endocranial anatomy ~~provide~~  
31  
32 information that helps to propose a taxonomic attribution for this fragment. Bone thickness shows  
33  
34 little variation. In modern humans, there is a clear decrease in bone thickness in the area of the  
35  
36 superior parietal gyrus. The pattern observed on this fragment resembles what has been described  
37  
38 for Neandertals (Balzeau, 2013). The position and size of the anterior branch of the meningeal  
39  
40 system on this fragment, as well as its subsequent bone thickness variation, fits with the anatomy  
41  
42 observed in Neandertals. The meningeal system in this area has more anastomoses than in modern  
43  
44 humans, and blood vessels are thinner and more numerous (Grimaud-Hervé, 1997). In summary the  
45  
46 anatomical features preserved in this parietal fragment are consistent with a Neandertal  
47  
48 classification.  
49  
50  
51

52  
53  
54  
55 The bone surface of the cranial ~~fragment~~~~remain~~ is well preserved and does not show  
56  
57 weathering (sensu Behrensmeyer, 1978). No direct carnivore activity (i.e., tooth marks) was  
58  
59 documented, nor any sign of burning. Similarly, no other biological modifications, such as rodent  
60

1 activity or root etching, was observed. This cranial fragment shows several striations in the outer  
2 table in five different areas (Figure 4). In some cases, the grooves are close “V” shaped, but  
3  
4 microstriations were not evident. On the other hand, the trajectories of the grooves are usually  
5  
6 sinuous and most of the bone surface is covered by very shallow striae. In some cases, the color of  
7  
8 the striations is lighter compared with the bone surface suggesting that they have occurred after its  
9  
10 deposition. These observations are compatible with trampling marks following the protocol  
11  
12 described by Domínguez-Rodrigo et al. (2009). Regarding the fracture analysis, this remain  
13  
14 displays three linear fractures, one of them parallel and two perpendicular to the cranial suture. The  
15  
16 two fractures perpendicular to the suture have right angled edges, jagged surfaces and absence of  
17  
18 cortical delamination. These characteristics are typical of fracturing in dry bone (Sala et al., 2016).  
19  
20 However, the fracture that is parallel to the suture displays an oblique angle, smooth surface and  
21  
22 presence of cortical delamination (0.75 cm) on the inner table. The combination of these fracture  
23  
24 attributes is usually considered representative of perimortem fractures (Sala et al., 2016).  
25  
26  
27  
28  
29  
30  
31  
32  
33

34 [INSERT FIGURE 4 HERE]  
35  
36  
37  
38

39 *3.2-Upper left fourth premolar, maxillary fragment with upper first molar and upper third molar*  
40  
41 *belonging to the same individual*  
42  
43  
44  
45

46 Descriptions and analyses are provided for the three dental remains belonging to the same  
47  
48 individual. These remains are shown in Figure 5 and are morphologically compared in Tables 3-5.  
49  
50  
51

52 Ax.13F.265.1 (AX.13E/13F.265-270.1 according to the museum records) is a complete  
53  
54 premolar, although its root is damaged and presents longitudinal cracks on both sides and some  
55  
56 smaller transversal cracks. In addition, there is a small pitting on the vestibular side of the buccal  
57  
58 cusp, and erosion on the tip of this cusp (Figure 5). Also, in the areas with the highest enamel  
59  
60

1  
2 thickness of the crown (the buccal and lingual sides) there is a part of the enamel that shows lower  
3  
4 density in the CT images ([Supplementary information Figure S12](#)). The similarity in height between  
5  
6 the lingual and buccal cusps and the two long inter-proximal facets suggest it is a P<sup>4</sup>. In addition,  
7  
8 the distal interproximal wear facet matches well the mesial counterpart of the Axlor M<sup>1</sup> ([Figure 5](#)),  
9  
10 further supporting that this is a P<sup>4</sup>, and indicating that they both belonged to the same individual  
11  
12 (see below).  
13  
14  
15  
16  
17

18 [INSERT FIGURE 5 HERE]  
19  
20  
21

22  
23 The occlusal surface is moderately worn (stage 3; Molnar, 1971), and the dentine is exposed  
24  
25 on the lingual cusp. Yet, the inter-proximal wear facets are visible to the naked eye, and the distal  
26  
27 one is larger. This premolar shows a distal accessory marginal tubercle, a bifurcated buccal essential  
28  
29 crest (grade 2 from Bailey, 2002) and a distal accessory ridge on the buccal cusp ([Table 3](#)).  
30  
31  
32  
33

34 [INSERT TABLE 3 HERE]  
35  
36  
37

38  
39 At the EDJ level, two major cusps are observed: buccal and lingual. The essential crest of  
40  
41 both the lingual and buccal cusps are bifurcated (Grade 2; [Table 3](#)), which are features typically  
42  
43 observed on Neandertals (92.3% and 61.5% respectively). On the mesial side it presents a  
44  
45 continuous transverse crest that does not connect with the horn tip of the lingual cusp, also typical  
46  
47 in Neandertals (69.2%). In addition, there is an intermediate accessory marginal tubercle distal to  
48  
49 the buccal cusp. The coronal pulp cavity is conformed by the two horns corresponding to the main  
50  
51 cusps, where the buccal horn is almost two times larger than the lingual one.  
52  
53  
54  
55

56  
57 This premolar shows a single, mediolaterally flat root. This root runs wide and straight in  
58  
59 the most cervical half, while the apical third is narrower. Both the mesial and distal sides present  
60



1  
2 longitudinal grooves, of which the distal is more pronounced. The analysis of the root canal based  
3  
4 on the  $\mu$ CT images shows that this is a single canal (Type 1R<sub>1</sub>) which is only found in 12.5% of  
5  
6 Neandertals (Pan & Zanolli, 2019; [Table 3](#)).  
7  
8  
9

10  
11 Geometric morphometric analyses show that Neandertals and recent modern humans are  
12  
13 almost completely separated along the P<sup>4</sup> morphospace, with Neandertals showing a lingually  
14  
15 expanded and asymmetric morphology and modern humans showing a symmetric and lingually  
16  
17 reduced configuration, where the interfoveal distance is strongly reduced ([Figure 6](#); Gómez-Robles  
18  
19 et al., 2011). Interestingly, fossil modern humans completely overlap with Neandertals, showing a  
20  
21 premolar configuration that is much more similar to that of Neandertals than to that of recent  
22  
23 modern humans. The Axlör P<sup>4</sup> plots right on the imaginary line that separates the areas of  
24  
25 distribution of Neandertals and recent modern humans, but outside the range of distribution of both  
26  
27 groups. The Axlör P<sup>4</sup> plots on this intermediate position because it shares a generally asymmetric  
28  
29 morphology with Neandertals, but a moderately reduced distal cusp and a shortened interfoveal  
30  
31 distance with modern humans. Based on these traits, a discriminant analysis classifies the Axlör P<sup>4</sup>  
32  
33 as a modern human, but with a low probability of only 56%. When adding size information, the  
34  
35 Axlör P<sup>4</sup> plots again in an intermediate position between Neandertals and recent modern humans.  
36  
37 Interestingly, it also plots on the lower extreme of the size variation found in fossil modern humans,  
38  
39 indicating that the Axlör P<sup>4</sup> is larger than most recent modern humans, but smaller than most  
40  
41 Neandertals and fossil modern humans.  
42  
43  
44  
45  
46  
47  
48  
49

50 [INSERT FIGURE 6 HERE]  
51  
52  
53  
54  
55  
56

57 Ax.13F.265.3 (AX.13E/13F.265-270.3 according to the museum records) represents a left  
58  
59 maxilla fragment, preserving both the external surface (ca. 13.3 × 9.2 mm), and the internal surface  
60

1  
2 (13.4 × 9.8 mm), with the left M<sup>1</sup> placed in its alveolus. This tooth is fragmented due to longitudinal  
3  
4 and transversal cracks that affect the crown and roots (Figure 5). Inter-proximal wear facets are  
5  
6 clear in both sides and the mesial one shows clear grooves on it. This mesial facet shows two  
7  
8 chippings in its occlusal border. Also, the occlusal surface of the tooth is heavily worn (stage 4-5;  
9  
10 Molnar, 1971) and the dentine is exposed in all four main cusps, which interferes with the  
11  
12 observation of several morphological traits.  
13  
14  
15  
16  
17

18 The metacone and the hypocone of this molar are well developed (grade 4 ASUDAS), and  
19  
20 there is no cusp 5 (Table 4). The hypocone is not distolingually projected, but it is aligned with the  
21  
22 protocone on the lingual side and with the metacone on the distal side. Due to the heavy occlusal  
23  
24 wear, it is not possible to score the presence of Carabelli's tubercle or the mesial marginal accessory  
25  
26 tubercle. The EDJ reveals the presence of an intermediate post-paracone tubercle and no sign of  
27  
28 fifth cusp (Table 4). Moreover, there is a type II *crista obliqua*, continuously connecting the  
29  
30 metacone to the protocone, which is centrally positioned. The occlusal wear also affects the dentine  
31  
32 to a large extent, which may influence trait assessments, but a Carabelli's tubercle does not seem to  
33  
34 be present. The horn tip of the hypocone pulp cavity is small and not projected, in contrast with the  
35  
36 typical Neandertal morphology (Supplementary Information Figure S14).  
37  
38  
39  
40  
41  
42

43 [INSERT TABLE 4 HERE]  
44  
45  
46  
47

48 The three roots are separated, all the radicular canals are divergent and the body is relatively  
49  
50 short. The canal corresponding to the mesio-buccal root is the widest one, being mesiodistally flat.  
51  
52 Moreover, the cervical third of this root canal is elongated, presenting a wide morphology, and the  
53  
54 apical end is bifurcated. This root morphology contrasts with the typical Neandertal taurodont  
55  
56 configuration.  
57  
58  
59  
60

1  
2 Analyses of shape variation show a generally clear separation between Neandertals and  
3  
4 modern humans, with Neandertals showing a skewed M<sup>1</sup> configuration and modern humans  
5  
6 showing a squared configuration ([Figure 6](#); Bailey, 2004; Gómez-Robles et al., 2007). Both groups  
7  
8 show a minor overlapping area where many fossil modern humans, as well as the Axlör M<sup>1</sup>, are  
9  
10 found. Based on shape data, Axlör M<sup>1</sup> is classified as a modern human with a probability of 88.8%  
11  
12 or 98.6% (before and after correcting the enamel cracks, respectively). Because of the small size of  
13  
14 the Axlör M<sup>1</sup>, adding size information to the PCA makes this specimen plot comfortably within the  
15  
16 modern human range of distribution.  
17  
18  
19  
20  
21

22  
23 When assessing only the M<sup>1</sup> outline as defined by curve semilandmarks ([Supplementary](#)  
24  
25 [Information Figure S15](#)), the differentiation between Neandertals and modern humans is less clear.  
26  
27 There is still an area of the morphospace occupied only for Neandertals and another one occupied  
28  
29 only by modern humans on the grounds of their skewed or squared outline configurations,  
30  
31 respectively. However, the overlapping area between both species is larger in this case.  
32  
33 Irrespectively of whether enamel cracks are corrected or not, the Axlör M<sup>1</sup> plots again in the area of  
34  
35 overlapping of both species. Outline shape data also classify the Axlör M<sup>1</sup> as a modern human with  
36  
37 a very high probability of more than 99% (with and without enamel crack corrections). Form  
38  
39 analyses (including size information) also make Axlör M<sup>1</sup> plot comfortably within the range of  
40  
41 variation of modern humans.  
42  
43  
44  
45  
46  
47  
48  
49

50 Ax.13F.265.2 (AX.13E/13F.265-270.2 according to museum records) This tooth is well  
51  
52 preserved upper left M<sup>3</sup>. The crown is complete, but the lingual root is broken, and it is possible to  
53  
54 observe longitudinal cracks on both sides of the preserved root fragment. In addition, it shows  
55  
56 moderate wear on the buccal cusp tips but there is no exposed dentine on them (stage 2; Molnar,  
57  
58 1971).  
59  
60

1  
2  
3  
4 There is a well-developed metacone but the hypocone is absent (Table 5). Nevertheless,  
5  
6 there is a small fifth cusp, that is positioned distally to a lingual tubercle. On the EDJ it can be  
7  
8 observed that there is no crista obliqua, and that the post-paracone tubercle is intermediate (Table  
9  
10 5). Dentine horn tips of the major cusps are not centrally compressed. The preserved part of the root  
11  
12 corresponds to the two buccal roots, with both apical tips completely closed. These two roots are  
13  
14 fused, but the root canals run independently along most of the root, except in the most apical tip  
15  
16 where they meet again.  
17  
18  
19  
20  
21

22 [INSERT TABLE 5 HERE]  
23  
24  
25  
26

27 Shape analyses show that the separation between Neandertal and modern human M<sup>3</sup>s is far  
28  
29 from clear (Figure 6; Gómez-Robles et al., 2012). Both species overlap completely along PC1, and  
30  
31 they show certain morphological trends only along PC2, with Neandertals tending to show positive  
32  
33 values associated with a more expanded hypocone, and modern humans tending to show negative  
34  
35 values associated with a strongly reduced hypocone that may be absent altogether. As with the other  
36  
37 adult posterior teeth, the M<sup>3</sup> from Axlor plots on the area of the morphospace where Neandertals  
38  
39 and modern humans overlap. Shape data classify this M<sup>3</sup> as a modern human with a probability of  
40  
41 78.4%, but it should be noted that the percentage of correct classification for Neandertals is very  
42  
43 low. The inclusion of size information makes this molar plot far outside the range of variation of  
44  
45 Neandertals on the grounds of its small size.  
46  
47  
48  
49  
50  
51

52 In summary, based on both morphological and size characteristics, this individual shows  
53  
54 stronger affinities with modern humans than with Neandertals.  
55  
56  
57  
58  
59  
60

### 3.3-Additional dental remains

AX.5B.299.16 This is a well-preserved lower right first incisor, although it shows heavy wear on the incisal edge, having lost between the 20-50% of the crown (roughly equivalent to Grade 4; Molnar, 1971; [Figure 7](#)). The degree of shoveling, labial convexity and the interproximal facets cannot be assessed due to the heavy incisal wear. The bucco-lingual diameter (7.7 mm) is larger than the one observed in modern humans and it fits well within the Neandertal range of variation. In contrast, the mesio-distal diameter is slightly smaller than the Neandertal minimum and falls within the modern human distribution ([Table 2](#)). Nonetheless, this mesio-distal measure is most probably affected by the wear of the crown. The cingular region is bulky, although there is no tuberculum dentale. The heavy wear also affects the observation of the degree of shoveling at the EDJ level, where no tuberculum dentale is observed. The root length of this incisor is 20.86 mm, equal to the maximum value reported in Neandertals (13.8-20.86 mm), and longer than the currently known values for Upper Palaeolithic (11.84-14.20 mm) and recent modern humans (13.18-19.22 mm) (comparative samples from Le Cabec et al., 2013). In addition, the root volume is higher than any reported value for Neandertals or anatomically modern humans (458.33 mm<sup>3</sup>). On the other hand, the volume of the crown pulp (CrPV) and the radicular canal (RpV) are in the low end of the variability of Neandertals, 6.61 mm<sup>3</sup> and 2.65 mm<sup>3</sup>, respectively. The ratio between the volume of these two values is 0.4, which is situated in the highest half of the Neandertal variability, indicating a proportionally bigger crown pulp segment compared to the root (comparative samples from Le Cabec et al., 2013). In sum, the features observed on this tooth (in particular, its crown and root length size) align it with Neandertals.

[INSERT FIGURE 7 HERE]

1  
2 AX.5B.299.31.64.17 This is an upper left first deciduous incisor with a well-preserved crown, but  
3  
4 the root is not complete (Figure 7). The smooth and twisted aspect of the fracture line of the root  
5  
6 has been interpreted in other individuals as the result of root resorption, corresponding to a 6-8-  
7  
8 years-old individual based on modern standards (AlQahtani, Hector, & Liversidge, 2010). Despite  
9  
10 the heavy wear (Grade 5, Molnar, 1971), a marked shovel shape is observable on the enamel  
11  
12 surface (>3 ASUDAS). The mesio-distal diameter of this incisor falls within the metric variation of  
13  
14 both Neandertals and modern humans, but the bucco-lingual diameter is larger than the maximum  
15  
16 value for the latter group (Table 2). There is no tuberculum dentale, and it is not possible to evaluate  
17  
18 the labial convexity on the enamel. The EDJ shows a strong and asymmetric labial convexity, more  
19  
20 marked on the mesial side than on the distal. Moreover, there is no tuberculum dentale observed at  
21  
22 the EDJ level, and it shows a well-developed shovel shape (>3 ASUDAS). In sum, the features  
23  
24 observed on this tooth (in particular, its strong and asymmetric labial convexity, its well-developed  
25  
26 shovel shape) and its size align it with Neandertals.  
27  
28  
29  
30  
31  
32  
33  
34  
35

36 AX.9E.283.103 This tooth is an upper left second deciduous molar that preserves a nearly complete  
37  
38 crown. The tooth is heavily worn exhibiting dentine in all four cusps, and the mesial inter-proximal  
39  
40 side of the enamel is missing. This tooth does not preserve the root, likely resorpted and/or  
41  
42 subsequently broken, and would have belonged to a 10-11-years-old individual based on modern  
43  
44 standards (AlQahtani et al., 2010). The size of the crown of this specimen does not provide  
45  
46 taxonomic information due to the large overlap between Neandertals and modern humans (Table 2).  
47  
48 Both the metacone and the hypocone are well developed (grade 4 ASUDAS). Despite the heavy  
49  
50 wear, it is possible to observe a big Carabelli's trait (Grade > 2 ASUDAS), but it is not possible to  
51  
52 assess the presence of any other accessory tubercles. The EDJ presents a big Carabelli's trait that is  
53  
54 affected by the fracture of the mesial interproximal side of the tooth, which does not allow locating  
55  
56 the dentine horn. Moreover, the crista obliqua is continuous, and of type II, with a centered placed  
57  
58  
59  
60

1  
2 protocone, which is a typical Neandertal trait (Becam et al., 2015; Becam & Chevalier, 2019). A  
3  
4 quantitative analysis of this molar has not been carried out, but qualitative observation shows that  
5  
6 the skewed morphology typical of Neandertal dm<sup>2</sup>s is not present (Bailey et al., 2014). A generally  
7  
8 squared outline morphology is present in this specimen instead. This squared morphology may  
9  
10 result from the presence of a well-developed Carabelli's trait, which is reported to give Neandertal  
11  
12 dm<sup>2</sup>s a less skewed appearance (Bailey et al., 2014). In sum, most features observed on this tooth  
13  
14 align it with Neandertals.  
15  
16  
17  
18  
19

## 20 **Discussion**

### 21 *Taxonomic assessment of the Axlor fossil remains*

22  
23  
24  
25  
26  
27  
28  
29 The human remains from Axlor can be divided into two different groups. The first group includes a  
30  
31 series of published dental remains, traditionally regarded as belonging to a single Neandertal  
32  
33 individual (Basabe, 1973), which our results better classify as belonging to a modern human.  
34  
35 Indeed, a detailed evaluation of the field notes of J.M. Barandiarán and our own assessment of the  
36  
37 stratigraphy at the place where these remains were found cast doubts regarding their belonging to  
38  
39 the Middle Paleolithic layers ([Supplementary Information Text S1](#)). The second group of human  
40  
41 remains includes three dental remains and a cranial fragment, described here for the first time,  
42  
43 which show clear Neandertal affinities and whose attribution to Mousterian layers seems secure  
44  
45 based on our assessment of the J.M. Barandiarán field notes.  
46  
47  
48  
49  
50

51  
52 The first group includes three teeth, P<sup>4</sup>, M<sup>1</sup> and M<sup>3</sup> (plus two additional lost specimens),  
53  
54 likely belonging to the same individual as already stated by Basabe (1973). The (moderate) wear  
55  
56 stage and the fact that the apical tip of the M<sup>3</sup> root is closed indicates that they belonged to a young  
57  
58 adult. Several features, mainly related to the M<sup>1</sup> morphology, question the previous taxonomic  
59  
60

1  
2 assignment of these teeth. First, the hypocone of the M<sup>1</sup> is not bulky and projected disto-lingually  
3  
4 (Figures 5-6; Supplementary Information Figures S14-S15), the tips of the dentine horns, as far as it  
5  
6 can be inferred given the heavy wear of the molar, are not centrally placed, and the molar is not  
7  
8 taurodont. In summary, this molar lacks all the traits that are typically associated with Neandertal  
9  
10 M<sup>1</sup>s. Second, the P<sup>4</sup> shows a single root channel (an infrequent trait in Neandertals; Pan & Zanolli,  
11  
12 2019), a reduced lingual cusp and a shortened interfoveal distance (typically observed in modern  
13  
14 humans). However, other traits in this individual seem to be more frequent in Neandertals. First, the  
15  
16 bifurcated buccal and lingual essential crests on the P<sup>4</sup> EDJ and the continuous transverse crest are  
17  
18 typically Neandertal features (Becam et al., 2019), as it is a generally asymmetric P<sup>4</sup> crown  
19  
20 (Gómez-Robles et al., 2011). Second, the presence of crista obliqua is a Neandertal M<sup>3</sup> common  
21  
22 feature (Martin et al., 2017), but the Axlör specimen does not present it in any typology. Moreover,  
23  
24 in this M<sup>3</sup> only the metacone dentine horn tip is slightly centrally placed, while the rest of the cusps  
25  
26 show the typical morphology of *Homo sapiens*. However, it should be noted that variation of  
27  
28 UPMH in many of these traits is not completely understood (e.g., for the P<sup>4</sup>, there is only  
29  
30 information from one UPMH; Becam et al., 2019). Moreover, the discovery of UPMH with  
31  
32 evidence of recent Neandertal admixture (Fu et al., 2015) and the mounting evidence that  
33  
34 Neandertal-modern human hybridization may have been common could partially explain the  
35  
36 differences found between the dental morphology of the UPMH and Holocene populations.  
37  
38  
39  
40  
41  
42  
43  
44

45 In addition, a qualitative assessment of the teeth that are now lost from the collection (C\*  
46  
47 and M<sup>2</sup>), based on the information and figures provided by Basabe (1973), indicates that they likely  
48  
49 belonged to the same individual due to the overall morphology and wear degree compatibility.  
50  
51 Moreover, the M<sup>3</sup> presents a small interproximal facet, compatible with the M<sup>2</sup> with reduced  
52  
53 hypocone presented by Basabe (1973). Regarding the morphology of these two lost teeth, it is  
54  
55 possible to observe on the original publication that the upper canine has some archaic features: a  
56  
57 bulky tuberculum linguale (ASUDAS grade >3) and well developed mesial ridge (grade 2), more  
58  
59  
60



1  
2 common in Neandertals (100% and 42.1%, respectively) and UPMHs (40% and 11.1%,  
3  
4 respectively) than in recent *Homo sapiens* (8% and 5.3%, respectively) (Martín-Torres et al.,  
5  
6 2012). On the other hand, the M<sup>2</sup> presents a large metacone (ASUDAS grade 3-4), a reduced  
7  
8 hypocone (ASUDAS grade 0-2), and absence of Carabelli's tubercle (ASUDAS grades 0-1).  
9  
10 Reduced hypocones are more common in UPMHs (50%) than in Neandertals (24.9%) (Martín-  
11  
12 Torres et al., 2012).  
13  
14

15  
16 Based on this morphological information, the absence of Holocene recent prehistory remains  
17  
18 from the Axlor sequence, the presence of an early Upper Paleolithic occupation in the site  
19  
20 (González-Urquijo et al., 2014), and the unclear previous ascription to the Mousterian level III due  
21  
22 to their finding in loose sediment close to the rock-shelter wall (see [Supplementary information](#)),  
23  
24 we hypothesize that these human remains could belong to an UPMH, which should be tested in the  
25  
26 near future using direct C14 datings. Currently, except for a few skeletons (Lagar Velho, Mirón;  
27  
28 Duarte et al., 1999; Carretero et al., 2015) most of the Upper Paleolithic remains from the Iberian  
29  
30 Peninsula consist of isolated teeth or cranial remains (Pérez Iglesias, 2007, and references therein).  
31  
32  
33

34  
35 We consider that the stratigraphic ascription of these teeth, rather than their morphology *per*  
36  
37 *se*, have contributed to incorrectly classify the published teeth from Axlor as belonging to  
38  
39 Neandertals. While Basabe (1973) considers that their general morphology resembles that of other  
40  
41 individuals found in Mousterian contexts, he still underlines their “evolved” status with the  
42  
43 presence of “intermediary characters” (Basabe, 1973:200), especially referring to the low degree of  
44  
45 taurodontism in the M<sup>1</sup> and the M<sup>2</sup>. The same author did classify the M<sup>1</sup> from Lezetxiki, which  
46  
47 shows the typical Neandertal occlusal morphology and a clear taurodontism (Basabe, 1970), as  
48  
49 belonging to a Neandertal individual.  
50  
51

52  
53 The second study that classified the Axlor teeth as Neandertals compared them with Sima de  
54  
55 los Huesos, Neandertals and modern humans both morphologically (using the data by Martín-  
56  
57 Torres et al., 2012) and metrically (using the data by Rodríguez-Cuenca (2003) and García-Bour,  
58  
59 Pérez-Pérez, & Chimenos (1997). However, most traits included in that study (Rostro-Carmona,  
60

1  
2 2013) are not taxonomically distinctive and, for those which are, the Axlor teeth show modern  
3  
4 human affinities. In terms of size, and using the data provided by Rostro-Carmona (2013), only the  
5  
6 canine would show a size closer to the Neandertal mean, the P<sup>4</sup> and M<sup>1</sup> would show intermediate  
7  
8 affinities while the size of the M<sup>2</sup> and M<sup>3</sup> would be more similar to modern humans. Our study  
9  
10 shows that, after including UPMHs in the comparative samples, and despite the overlap between  
11  
12 modern humans and Neandertals, the general size of the Axlor teeth is either non-determinant or  
13  
14 more similar to modern humans. Finally, Rostro-Carmona (2013) used the presence of taurodontism  
15  
16 in the Axlor teeth to classify them as belonging to Neandertals, but our assessment indicates that the  
17  
18 Axlor teeth show a very limited degree of taurodontism, particularly when compared with classic  
19  
20 Neandertal molars.  
21  
22  
23  
24

25 The second group would encompass the cranial fragment and three additional tooth remains  
26  
27 that have clear Neandertal affinities and their stratigraphic position is secure within the Mousterian  
28  
29 levels. The bone thickness distribution pattern and endocranial anatomy of the cranial  
30  
31 fragment remain are consistent with Neandertal anatomy. Additionally, both incisors and the dm<sup>2</sup>  
32  
33 present characteristics that allow us to ascribe them to Neandertals. Although heavily worn, the I<sub>1</sub>  
34  
35 shows Neandertal affinities in its root configuration and proportions. Nevertheless, the CrPV and  
36  
37 RpV values are lower than the Neandertal values reported to date (Le Cabec et al., 2013; Becam &  
38  
39 Chevalier, 2019). This might be related to an advanced age for the individual, as aging related  
40  
41 deposition of secondary dentine causes the reduction of the pulp channel (Aboshi, Takahashi, &  
42  
43 Komuro, 2010; Solheim, 1992). This would be consistent with the heavy wear present in this tooth.  
44  
45 Second, both the OES and EDJ of the deciduous upper incisor from Axlor present a set of  
46  
47 characteristics observed in other Neandertal specimens such as Portel-Ouest, La Ferrassie 8 (strong  
48  
49 mesial and distal marginal ridges, pronounced and asymmetric labial convexity) (Becam &  
50  
51 Chevalier, 2019). Third, although the dm<sup>2</sup> does not show the typical Neanderthal skewed  
52  
53 configuration, it does show a notable development of the hypocone in relation to the metacone, the  
54  
55 presence of the crista obliqua, and a large Carabelli's tubercle at the OES and EDJ. These are  
56  
57  
58  
59  
60

1  
2 common features to other Neandertal dm<sup>2</sup>s, such as Arrillor, La Ferrassie 8 or Portel-Ouest (Becam  
3  
4 & Chevalier, 2019; Bermúdez de Castro & Saenz de Buruaga, 1999). These new remains confirm  
5  
6 the presence of Neandertal fossil remains in Axlor, thus increasing the Neandertal hypodigm  
7  
8 recovered in the Eastern Cantabrian Region.  
9

### 10 11 12 13 14 15 16 *Origin of the accumulation of the human fossil remains* 17 18 19

20 Taphonomic and forensic analyses on hominin fossils are important to determine the origin of  
21  
22 bone deposition and reconstruct the processes occurred during the fossil-diagenetic processes even  
23  
24 for isolated fossils (Sanz et al., 2018). In some cases, it is even possible to determine causes of  
25  
26 death (Sala et al., 2015) or drawing inferences about the mortuary practices of hominin groups, such  
27  
28 as cannibalism (Rougier et al., 2016; Sala & Conard, 2016; Saladié et al., 2012; Saladié &  
29  
30 Rodríguez-Hidalgo, 2017) or funerary activities (Gómez-Olivencia et al., 2018b).  
31  
32  
33  
34  
35

36 In the case of the two deciduous teeth, they were lost by two different Neandertal individuals  
37  
38 during the formation of levels V (left di<sup>1</sup>) and IV (right dm<sup>2</sup>). The presence of isolated deciduous  
39  
40 teeth is not rare in Middle Paleolithic layers, and the closest example is found less than 25 km south  
41  
42 from Axlor, in Arrillor (Figure 1; Bermúdez de Castro & Saénz de Buruaga, 1999; Iriarte-  
43  
44 Chiapusso, Wood, & Sáenz de Buruaga, 2019), with other example from Le Portel Ouest (Becam &  
45  
46 Chevalier, 2019). The cranial fragment from Axlor displays evidence of postmortem and  
47  
48 perimortem fractures, but the absence of traces that could indicate the causes of such fractures  
49  
50 makes it difficult to interpret its origin. Although we cannot rule out intentional causes for the  
51  
52 perimortem fractures, the lack of clear anthropic cut marks or signs of anthropic manipulation does  
53  
54 not allow us to go further in our interpretation. The absence of weathering could be interpreted as a  
55  
56 non-aerial (or short-term) exposure of the fossils in the biostratigraphic phase. On the other hand,  
57  
58  
59  
60

1  
2 trampling has been documented on the cranial fragment suggesting certain displacement of the  
3  
4 fossils which could be one of the explanations of the scarcity of human remains at the site.  
5  
6 Additionally, the Barandiarán collection shows some significant bias in comparison with the  
7  
8 richness in fossil remains that we have observed at the site during recent excavations (Gómez-  
9  
10 Olivencia et al., 2018a), in which smaller shaft fragments are absent. This bias could be a secondary  
11  
12 reason of this scarcity. In this context, the recovery of additional human fossils in the Axlor site  
13  
14 would help elucidate the nature of these isolated remains found in a human occupation context.  
15  
16  
17  
18  
19

## 20 **Conclusions**

21  
22 Axlor (Dima, Biscay) is one of the most important Middle Paleolithic sites in the Cantabrian  
23  
24 region (northern Iberian Peninsula). The excavations performed by J.M. Barandiarán at the Axlor  
25  
26 site 50 years ago yielded a cranial vault fragment and eight teeth, five of which likely belonged to  
27  
28 the same individual, although two are currently lost. Three teeth (a left  $dm^2$ , a left  $di^1$ , and a right  $I_1$ )  
29  
30 and the cranial fragment show morphological features consistent with their classification as  
31  
32 Neandertals, and were found in undisturbed Mousterian context. However, the remaining three teeth  
33  
34 (plus two that have been lost since the initial finding), traditionally classified as Neandertals  
35  
36 (Basabe, 1973; Rostro Carmona, 2013), show morphological features and a general size more  
37  
38 compatible with their classification as modern humans. Moreover, the review of the original notes  
39  
40 by J.M. Barandiarán and our own observations during the recent excavations at the site suggest that  
41  
42 the archaeological context of these remains should be carefully reconsidered. We hypothesize that  
43  
44 these teeth may constitute one of the scarce examples of Upper Paleolithic remains in the Iberian  
45  
46 Peninsula, a hypothesis that would require a direct C14 dating to be tested, which currently is not  
47  
48 possible due to access limitations.  
49  
50  
51  
52  
53

## 54 **ACKNOWLEDGMENTS**

55  
56  
57  
58  
59  
60

1 We would like to thank I. García Camino (Arkeologi Museoa) for permission to study these  
2 fossils. We thank L. García Boullosa for the cleaning of some of these fossils, and to the rest of the  
3 Arkeologi Museoa staff. The Gobierno Vasco-Eusko Jaurlaritzza granted the permission to micro-CT  
4 these specimens. Thanks to the Jose Miguel de Barandiaran Fundazioa and Zuriñe Velez de  
5 Mendizabal for the access to J.M. de Barandiarán's field notes. Thanks to B. Notario (CENIEH) for  
6 help during the micro-CT scanning process. This research has also received support from the  
7 Spanish Ministerio de Ciencia, Innovación y Universidades (proyecto PGC2018-093925-B-C33),  
8 Research Group IT1418-19 from the Eusko Jaurlaritzza-Gobierno Vasco. AGO was supported by  
9 Ramón y Cajal fellowship (RYC-2017-22558). NS was supported by a Juan de la Cierva  
10 Incorporación program (IJCI-2017-32804). Thanks also to our colleagues from BBP, UCM-ISCIH,  
11 EHU-UPV, as well as to A. Rodríguez-Hidalgo and N. Weaver for stimulating discussions.

### **Data Availability Statement**

The original micro-ct scans, the derived segmentation files, and 3D volumes are available in  
figshare at <https://doi.org/10.6084/m9.figshare.10308272>.

### **ORCID**

*Asier Gómez-Olivencia* <https://orcid.org/0000-0001-7831-3902>

*Diego López-Onaindia* <https://orcid.org/0000-0002-5266-6416>

*Nohemi Sala* <https://orcid.org/0000-0002-0896-1493>

*Antoine Balzeau* <https://orcid.org/0000-0002-4226-611X>

*Ana Pantoja-Pérez* <https://orcid.org/0000-0001-9302-1756>

*Ana Pantoja*

*Ignacio Arganda-Carreras* <https://orcid.org/0000-0003-0229-5722>

*Mikel Arlegi* <http://orcid.org/0000-0001-5665-9275>

*Joseba Rios-Garaizar* <https://orcid.org/0000-0001-8474-2156>

1  
2 Aida Gómez-Robles <https://orcid.org/0000-0002-8719-2660>  
3  
4  
5  
6  
7

8  
9 **REFERENCES**  
10

- 11  
12  
13 Aboshi, H., Takahashi, T., & Komuro, T. (2010). Age estimation using microfocus X-ray computed  
14 tomography of lower premolars. *Forensic Science International*, *200*, 35-40.  
15  
16  
17  
18 Albisu Andrade, C., Etxeberria Gabilondo, F., & Herrasti Erlogorri, L. (2014). Estudio de los restos  
19 dentales humanos procedentes de la cueva de Santa Catalina. In E. Berganza Gochi, & J. L.  
20 Arribas Pastor (Eds.). *La Cueva de Santa Catalina (Lekeitio): La intervención arqueológica*  
21 *Restos vegetales, animales y humanos*, (pp. 361-365). Bilbao: Bizkaiko Foru Aldundia.  
22  
23  
24  
25  
26  
27 Altuna, J. (1989). La subsistance d'origine animal pendant le Moustérien dans la région Cantabrique  
28 (Espagne). In M. Pathou, & L. G. Freeman (Eds.). *L'Homme de Neandertal La Subsistance*  
29 *Actes du Colloque International de Liège*, vol 6, (pp. 41-43). Liège: ERAUL.  
30  
31  
32  
33  
34 AlQahtani, S.J., Hector, M.P., & Liversidge, H.M. (2010). The London atlas of human tooth  
35 development and eruption. *American Journal of Physical Anthropology*, *142*, 481-490.  
36  
37  
38  
39 ~~Arambourou, R., & Genet Varcin, R. (1965). Nouvelle sépulture du Magdalénien final dans la~~  
40 ~~grotte Duruthy à Sorde-l'Abbaye (Landes): Masson.~~  
41  
42  
43  
44 Arganda-Carreras, I., Kaynig, V., Rueden, C., Schindelin, J., Eliceiri, K. W., Cardona, A., &  
45 Sebastian Seung, H. (2017). Trainable Weka Segmentation: a machine learning tool for  
46 microscopy pixel classification. *Bioinformatics*, *33*, 2424-2426.  
47  
48  
49  
50 Bayle, P., Le Luyer, M., & Robson Brown, K. A. (2017). The Palomas Dental Remains: Thickness  
51 and Tissue Proportions. In E. Trinkaus, & M. J. Walker (Eds.). *Neandertals from the Sima*  
52 *de las Palomas del Cabezo Gordo, Southeastern Spain*, (pp. 115-137). College Station,  
53 Texas: Texas A&M University Press.  
54  
55  
56  
57  
58  
59  
60

- 1  
2 Bailey, S. E. (2002). A closer look at Neanderthal postcanine dental morphology: The mandibular  
3  
4 dentition. *The Anatomical Record*, 269, 148-156.  
5
- 6 Bailey, S. E. (2004). A morphometric analysis of maxillary molar crowns of Middle-Late  
7  
8 Pleistocene hominins. *Journal of Human Evolution*, 47, 183-198.  
9
- 10 Bailey, S. E., Benazzi, S., Souday, C., Astorino, C., Paul, K., & Hublin, J.-J. (2014). Taxonomic  
11  
12 differences in deciduous upper second molar crown outlines of *Homo sapiens*, *Homo*  
13  
14 *neanderthalensis* and *Homo erectus*. *Journal of Human Evolution*, 72, 1-9.  
15
- 16 Balzeau, A. (2013). Thickened cranial vault and parasagittal keeling: Correlated traits and  
17  
18 autapomorphies of *Homo erectus*? *Journal of Human Evolution*, 64, 631-644.  
19
- 20 Balzeau, A., Buck, L. T., Albessard, L., Becam, G., Grimaud-Hervé, D., Rae, T. C., & Stringer, C.  
21  
22 B. (2017). The Internal Cranial Anatomy of the Middle Pleistocene Broken Hill 1 Cranium.  
23  
24 *PaleoAnthropology*, 2017, 107-138.  
25
- 26 Balzeau, A., Grimaud-Hervé, D., & Gilissen, E. (2011). Where are inion and endinion? Variations  
27  
28 of the exo- and endocranial morphology of the occipital bone during hominin evolution.  
29  
30 *Journal of Human Evolution*, 61, 488-502.  
31
- 32 Barandiarán, I., & Cava, A. (2008). Identificaciones del Gravetiense en las estribaciones  
33  
34 occidentales del Pirineo: modelos de ocupación y uso. *Trabajos de Prehistoria*, 65, 13-28.  
35
- 36 Barandiarán, J. M. (1980). Excavaciones en Axlor. 1967-1974. In J. M. Barandiarán (Ed.). *Obras*  
37  
38 *Completas de José Miguel de Barandiarán Tomo XVII*, (pp. 127-384). Bilbao: La Gran  
39  
40 Enciclopedia Vasca.  
41
- 42 Basabe, J. M. (1970). Dientes humanos del paleolítico de Lezetxiki (Mondragón). *Munibe*, XXII,  
43  
44 113-124.  
45
- 46 Basabe, J. M. (1973). Dientes humanos del Musteriense de Axlor (Dima. Vizcaya). *Trabajos de*  
47  
48 *Antropología*, 16, 187-207.  
49
- 50 Basabe, J. M. (1982). Restos fósiles humanos de la región Vasco-Cantábrica. *Cuadernos de Sección*  
51  
52 *Antropología-Etnografía*, 1, 67-84.  
53  
54  
55  
56  
57  
58  
59  
60

- 1  
2 Becam, G., Chevalier, T., Gregoire, S., Braga, J., Balzeau, A., De Lumley, M.A., Veizian, R. 2015.  
3  
4 The characterization of the outer enamel surface and the enamel dentine junction of  
5  
6 deciduous and permanent Neandertal teeth from Le Portel-Ouest cave (Ariège, France).  
7  
8 *1840<sup>ème</sup> Journée de la Société d'Anthropologie de Paris*.  
9  
10  
11 Becam, G., & Chevalier, T. (2019). Neandertal features of the deciduous and permanent teeth from  
12  
13 Portel-Ouest Cave (Ariège, France). *American Journal of Physical Anthropology*, 168, 45-  
14  
15 69.  
16  
17  
18 Becam, G., Verna, C., Gómez-Robles, A., Gómez-Olivencia, A., Albessard, L., Arnaud, J., . . .  
19  
20 Balzeau, A. (2019). Isolated teeth from La Ferrassie: Reassessment of the old collections,  
21  
22 new remains, and their implications. *American Journal of Physical Anthropology*, 169, 132-  
23  
24 142.  
25  
26  
27 Behrensmeyer, A. K. (1978). Taphonomic and ecologic information from bone weathering.  
28  
29 *Paleobiology*, 4, 150-162.  
30  
31  
32 Bermúdez de Castro, J. M., & Sáenz de Buruaga, A. (1999). Étude Préliminaire du site Pléistocène  
33  
34 Supérieur à hominidé d'Arrillor (Pays Basque, Espagne). *L'Anthropologie*, 103, 633-639.  
35  
36  
37 Carlsen, O. (1987). Dental Morphology. Copenhagen: Munksgaard.  
38  
39 Carretero, J. M., Quam, R. M., Gómez-Olivencia, A., Castilla, M., Rodríguez, L., & García-  
40  
41 González, R. (2015). The Magdalenian human remains from El Mirón Cave, Cantabria  
42  
43 (Spain). *Journal of Archaeological Science*, 60, 10-27.  
44  
45  
46 Castaños, P. M. (2005). Revisión actualizada de las faunas de macromamíferos del Würm antiguo  
47  
48 en la Región Cantábrica. In J. A. Lasheras, & R. Montes (Eds.). Neandertales cantábricos,  
49  
50 estado de la cuestión, (pp. 201-207). Santander: Museo de Altamira.  
51  
52  
53 de la Rúa, C., & Hervella, M. (2011). Estudio antropológico de los dientes humanos de la cueva de  
54  
55 Aitzbitarte III (Rentería. Gipuzkoa) (Paleolítico superior). In J. Altuna, K. Mariezkurrena, &  
56  
57 J. Rios (Eds.). Ocupaciones humanas en Aitzbitarte III (País Vasco) 33600-18400 BP (Zona  
58  
59 de entrada a la cueva), (pp. 385-393). Vitoria-Gasteiz: Eusko Jaurlaritza-Gobierno Vasco.  
60



- 1  
2 Domínguez-Rodrigo, M., de Juana, S., Galán, A. B., & Rodríguez, M. (2009). A new protocol to  
3  
4 differentiate trampling marks from butchery cut marks. *Journal of Archaeological Science*,  
5  
6 36, 2643-2654.  
7  
8  
9 Duarte, C., Maurício, J., Souto, P., Pettitt, P. B., Trinkaus, E., Van Plicht, H. D., & Zilhão, J.  
10  
11 (1999). The early Upper Paleolithic human skeleton from the Abrigo do Lagar Velho  
12  
13 (Portugal) and modern human emergence in Iberia. *Proceedings of the National Academy of*  
14  
15 *Sciences of the United States of America*, 96, 7604-7609.  
16  
17  
18 Fu, Q., Hajdinjak, M., Moldovan, O. T., Constantin, S., Mallick, S., Skoglund, P., . . . Pääbo, S.  
19  
20 (2015). An early modern human from Romania with a recent Neanderthal ancestor. *Nature*,  
21  
22 524, 216-219.  
23  
24  
25 García-Bour, J., Pérez-Pérez, A., & Chimenos, E. (1997). Evolución de la dentición en la transición  
26  
27 mesolítico-neolítico de la península ibérica; un modelo de sustitución poblacional. *Anales*  
28  
29 *de Odontostomatología*, 3, 116-121.  
30  
31  
32 Garralda, M. D. (2005). Los Neandertales en la Península Ibérica. *Munibe (Antropología*  
33  
34 *Arkeologia)*, 57, 289-314.  
35  
36  
37 Garralda, M.-D., Maíllo-Fernández, J.-M., Higham, T., Neira, A., & Bernaldo de Quirós, F. (in  
38  
39 press). The Gravettian child mandible from El Castillo Cave (Puente Viesgo, Cantabria,  
40  
41 Spain). *American Journal of Physical Anthropology*. <https://doi.org/10.1002/ajpa.23906>  
42  
43  
44 Gómez-Olivencia, A., Quam, R., Sala, N., Bardey, M., Ohman, J. C., & Balzeau, A. (2018b). La  
45  
46 Ferrassie 1: New perspectives on a “classic” Neandertal. *Journal of Human Evolution*, 117,  
47  
48 13-32.  
49  
50  
51 Gómez-Olivencia, A., Sala, N., Núñez-Lahuerta, C., Sanchis, A., Arlegi, M., & Rios-Garaizar, J.  
52  
53 (2018a). First data of Neandertal bird and carnivore exploitation in the Cantabrian Region  
54  
55 (Axlor; Barandiaran excavations; Dima, Biscay, Northern Iberian Peninsula). *Scientific*  
56  
57 *Reports*, 8, 10551.  
58  
59  
60

- 1  
2 Gómez-Robles, A., Bermúdez de Castro, J. M., Martínón-Torres, M., Prado-Simón, L., & Arsuaga,  
3  
4 J. L. (2012). A geometric morphometric analysis of hominin upper second and third molars,  
5  
6 with particular emphasis on European Pleistocene populations. *Journal of Human*  
7  
8 *Evolution*, 63, 512-526.  
9
- 10 Gómez-Robles, A., Martínón-Torres, M., Bermúdez de Castro, J. M., Margvelashvili, A., Bastir,  
11  
12 M., Arsuaga, J. L., . . . Martínez, L. M. (2007). A geometric morphometric analysis of  
13  
14 hominin upper first molar shape. *Journal of Human Evolution*, 53, 272-285.  
15  
16
- 17 Gómez-Robles, A., Martínón-Torres, M., Bermúdez de Castro, J. M., Prado-Simón, L., & Arsuaga,  
18  
19 J. L. (2011). A geometric morphometric analysis of hominin upper premolars. Shape  
20  
21 variation and morphological integration. *Journal of Human Evolution*, 61, 688-702.  
22  
23
- 24 González Echegaray, J., & Freeman, L. G. (1973). Cueva Morín: Excavaciones 1969. Santander:  
25  
26 Publicaciones del Patronato de las Cuevas Prehistóricas de la Provincia de Santander.  
27  
28
- 29 González Echegaray, J., García Guinea, M. A., Begines Ramírez, A., & Madariaga de la Campa, B.  
30  
31 (1963). Cueva de la Chora (Santander). Madrid: Ministerio de Educación Nacional.  
32  
33 Dirección General de Bellas Artes. Servicio Nacional de Excavaciones Arqueológicas.  
34  
35
- 36 González Echegaray, J., & Ripoll Perelló, E. (1954). Hallazgos en la cueva de La Pasiega (Puente  
37  
38 Viesgo, Santander). *Ampurias*, XV-XVI, 43-65.  
39  
40
- 41 González-Urquijo, J. E., Ibañez, J. J., Lazuén, T., & Mozota, M. (2014). Axlor. In R. Sala (Ed.).  
42  
43 Los Cazadores Recolectores Del Pleistoceno Y Del Holoceno En Iberia Y El Estrecho de  
44  
45 Gibraltar, (pp. 45-48). Burgos: Universidad de Burgos.  
46  
47
- 48 Grimaud-Hervé, D. (1997). L'évolution de l'encéphale chez *Homo erectus* et *Homo sapiens*:  
49  
50 exemples de l'Asie et de l'Europe: CNRS ed. Paris.  
51
- 52 Guerrero Sala, L. A., & Lorenzo Lizalde, J. L. (1981). Antropología física en Rascaño. In J.  
53  
54 González Echegaray, & I. Barandiarán Maestu, (Eds.), *El Paleolítico Superior de la Cueva*  
55  
56 *de Rascaño (Santander)* (pp. 278-). Santander: Ministerio de Cultura. Dirección General de  
57  
58 Bellas Artes, Archivos y Bibliotecas.  
59  
60

1  
2 Henry-Gambier, D. (2006). Les sépultures de Sorde-l'Abbaye (Landes). In M. Dachary, (Ed.), *Les*  
3 *Magdaléniens à Duruthy Qui étaient-ils, comment vivaient-ils?* (pp. 67-73). Mont-de-  
4 *Marsan: Conseil général des Landes.*  
5  
6  
7

8  
9 Henry-Gambier, D., Normand, C., & Pétilion, J.-M. (2013). Datation radiocarbone directe et  
10 attribution culturelle des vestiges humains paléolithiques de la grotte d'Isturitz (Pyrénées-  
11 Atlantiques). *Bulletin de la Société préhistorique française*, 110, 645-656.  
12  
13

14  
15 Iriarte-Chiapusso, M. J., Wood, R., & Sáenz de Buruaga, A. (2019). Arrillor cave (Basque Country,  
16 northern Iberian Peninsula). Chronological, palaeo-environmental and cultural notes on a  
17 long Mousterian sequence. *Quaternary International*, 508, 107-115.  
18  
19

20  
21 Jarvis, A., Reuter, H. I., Nelson, A., & Guevara, E. (2008). Hole-filled SRTM for the globe Version  
22 4. available from the CGIAR-CSI SRTM 90m Database (<http://srtm.csi.cgiar.org>), 15, 25-  
23 54.  
24  
25  
26  
27

28  
29 Le Cabec, A., Gunz, P., Kupczik, K., Braga, J., & Hublin, J.-J. (2013). Anterior tooth root  
30 morphology and size in Neanderthals: Taxonomic and functional implications. *Journal of*  
31 *Human Evolution*, 64, 169-193.  
32  
33  
34

35  
36 Legland, D., Arganda-Carreras, I., & Andrey, P. (2016). MorphoLibJ: integrated library and plugins  
37 for mathematical morphology with ImageJ. *Bioinformatics*, 32, 3532-3534.  
38  
39

40  
41 Marín-Arroyo, A. B., Rios-Garaizar, J., Straus, L. G., Jones, J. R., de la Rasilla, M., González  
42 Morales, M. R., . . . Ocio, D. (2018). Chronological reassessment of the Middle to Upper  
43 Paleolithic transition and Early Upper Paleolithic cultures in Cantabrian Spain. *Plos one*, 13,  
44 e0194708.  
45  
46  
47  
48

49  
50 Martin, R. M. G., Hublin, J.-J., Gunz, P., & Skinner, M. M. (2017). The morphology of the enamel-  
51 dentine junction in Neanderthal molars: Gross morphology, non-metric traits, and temporal  
52 trends. *Journal of Human Evolution*, 103, 20-44.  
53  
54  
55  
56  
57  
58  
59  
60

- 1  
2 Martínón-Torres, M., Bermúdez de Castro, J. M., Gómez-Robles, A., Prado-Simón, L., & Arsuaga,  
3  
4 J. L. (2012). Morphological description and comparison of the dental remains from  
5  
6 Atapuerca-Sima de los Huesos site (Spain). *Journal of Human Evolution*, *62*, 7-58.  
7  
8  
9 Molnar, S. (1971). Human tooth wear, tooth function and cultural variability. *American Journal of*  
10  
11 *Physical Anthropology*, *34*, 175-190.  
12  
13 Obermaier, H. (1925). *El hombre fósil*. Madrid: Ediciones Istmo.  
14  
15 Pan, L., & Zanolli, C. (2019). Comparative observations on the premolar root and pulp canal  
16  
17 configurations of Middle Pleistocene Homo in China. *American Journal of Physical*  
18  
19 *Anthropology*, *168*, 637-646.  
20  
21  
22 Pérez-Iglesias, J. M. (2007). Restos fósiles humanos en el Paleolítico superior de la península  
23  
24 ibérica. *Arqueoweb*, *8*, 1-17.  
25  
26  
27 QGIS Development Team, 2009. QGIS Geographic Information System. Open Source Geospatial  
28  
29 Foundation. URL <http://qgis.org>  
30  
31  
32 Rios-Garaizar, J. (2017). A new chronological and technological synthesis for Late Middle  
33  
34 Paleolithic of the Eastern Cantabrian Region. *Quaternary International*, *433*, 50-63.  
35  
36 Rodríguez Cuenca, J. V. (2003). *Dientes y diversidad humana: avances de la antropología dental*.  
37  
38 Bogotá: Editora Guadalupe Ltda.  
39  
40  
41 Rostro Carmona, J. (2013). Estudio comparado de las piezas dentales de *Homo neanderthalensis* del  
42  
43 yacimiento Musteriense de Axlor (Dima, Vizcaya). *CKQ Estudios de*  
44  
45 *Cuaternario/Kuaternario Ikasketak/Quaternary Studies*, *3*, 91-100.  
46  
47  
48 Rougier, H., Crevecoeur, I., Beauval, C., Posth, C., Flas, D., Wißing, C., . . . Krause, J. (2016).  
49  
50 Neandertal cannibalism and Neandertal bones used as tools in Northern Europe. *Scientific*  
51  
52 *Reports*, *6*, 29005.  
53  
54  
55 Sala, N., & Conard, N. (2016). Taphonomic analysis of the hominin remains from Swabian Jura and  
56  
57 their implications for the mortuary practices during the Upper Paleolithic. *Quaternary*  
58  
59 *Science Reviews*, *150*, 278-300.  
60

- 1  
2 Sala, N., Pantoja-Pérez, A., Arsuaga, J. L., Pablos, A., & Martínez, I. (2016). The Sima de los  
3  
4 Huesos Crania: Analysis of the cranial breakage patterns. *Journal of Archaeological*  
5  
6 *Science*, 72, 25-43.  
7  
8  
9 Saladié, P., Huguet, R., Rodríguez-Hidalgo, A., Cáceres, I., Esteban-Nadal, M., Arsuaga, J. L., . . .  
10  
11 Carbonell, E. (2012). Intergroup cannibalism in the European Early Pleistocene: The range  
12  
13 expansion and imbalance of power hypotheses. *Journal of Human Evolution*, 63, 682-695.  
14  
15  
16 Saladié, P., & Rodríguez-Hidalgo, A. (2017). Archaeological Evidence for Cannibalism in  
17  
18 Prehistoric Western Europe: from Homo antecessor to the Bronze Age. *Journal of*  
19  
20 *Archaeological Method and Theory*, 24, 1034-1071.  
21  
22  
23 Sanguino González, J., & Montes Barquín, r. (2005). Nuevos datos para el conocimiento del  
24  
25 Paleolítico Medio en el centro de la Región Cantábrica: la cueva de Covalejos (Piélagos,  
26  
27 Cantabria). In R. Montes Barquín, & J. A. Lasheras Corruchaga, (Eds.), *Actas de la Reunión*  
28  
29 *científica: Neandertales cantábricos, estado de la cuestión* (pp. 489-538). Santander: Museo  
30  
31 Nacional y Centro de Investigación de Altamira. Ministerio de Cultura.  
32  
33  
34 Sanz M., Sala N., Daura J., Pantoja-Pérez A., Santos E, Zilhão J, and Arsuaga JL. (2018).  
35  
36 Taphonomic inferences about Middle Pleistocene hominins: The human cranium of Gruta  
37  
38 da Aroeira (Portugal). *American Journal of Physical Anthropology*, 167, 615-627.  
39  
40  
41 Schindelin, J., Arganda-Carreras, I., Frise, E., Kaynig, V., Longair, M., Pietzsch, T., . . . Cardona,  
42  
43 A. (2012). Fiji: an open-source platform for biological-image analysis. *Nature Methods*,  
44  
45 9,676.  
46  
47  
48 Solheim, T. (1992). Amount of secondary dentin as an indicator of age. *European Journal of Oral*  
49  
50 *Sciences*, 100, 193-199.  
51  
52  
53 Tejero, J. M., Avezuela, B., White, R., Ranlett, S., Quam, R., Tattersall, I., & Bernaldo de Quirós,  
54  
55 F. (2010). Un pedazo de la Prehistoria cántabra en Nueva York. Las Colecciones de la  
56  
57 Cueva de El Castillo (Puente Viesgo, Cantabria) en el American Museum of Natural History  
58  
59 (Nueva York, EEUU). *Munibe (Antropología-Arkeología)*, 61, 5-16.  
60

1  
2 Turner, C. G., Nichol, C. R., & Scott, G. R. (1991). Scoring procedures for key morphological traits  
3  
4 of the permanent dentition: the Arizona State University dental anthropology system. In M.  
5  
6 Kelley, & C. Larsen (Eds.). *Advances in Dental Anthropology*, (pp. 13-31). New York:  
7  
8 Wiley-Liss.  
9

10  
11 Vallois, H., & Delmas, L. (1976). Los frontales de la cueva de El Castillo (España). *Trabajos de*  
12  
13 *Prehistoria*, 33, 113-120.  
14

15  
16 Zapata, J., Bayle, P., Lombardi, A. V., Pérez-Pérez, A., & Trinkaus, E. (2017). The Palomas Dental  
17  
18 Remains: Preservation, Wear, and Morphology. In E. Trinkaus, & M. J. Walker (Eds.),  
19  
20 *Neandertals from the Sima de las Palomas del Cabezo Gordo, Southeastern Spain* (pp. 52-  
21  
22 88). College Station, Texas: Texas A&M University Press.  
23  
24  
25  
26  
27  
28  
29  
30  
31  
32  
33  
34  
35  
36  
37  
38  
39  
40  
41  
42  
43  
44  
45  
46  
47  
48  
49  
50  
51  
52  
53  
54  
55  
56  
57  
58  
59  
60

## Figure legends

**FIGURE 1** Location of Axlor (red star) and other Paleolithic sites with human remains in the Center and East of the Cantabrian Region (northern Iberian Peninsula and southwestern France). 1: La Pasiega (González Echegaray & Ripoll Perelló, 1954); 2: Castillo (N; HS; Garralda, 2005; Garralda, Maíllo-Fernández, Higham, Neira, & Bernaldo de Quirós, in press; Obermaier, 1925; Tejero et al., 2010; Vallois & Delmas, 1976; 3 Covalejos (N, HS; Sanguino González & Montes Barquín, 2005); 4: Pendo (Basabe, 1982); 5: Morín (HS; González Echegaray & Freeman, 1973; Obermaier, 1925); 6: Rascaño (Guerrero Sala & Lorenzo Lizalde, 1981); 7: La Chora (González Echegaray, García Guinea, Begines Ramírez & Madariaga de la Campa, 1963); 8: Mirón (HS; Carretero et al., 2015); 9: Arrillor (N, Bermúdez de Castro & Sáenz de Buruaga, 1999); 10: Axlor (N; HS; this work); 11: Lezetxiki (N; Basabe, 1970); 12: Santa Catalina (HS; Albisu Andrade, Etxeberria Gabilondo, & Herrasti Erlogorri, 2014); 13: Aitzbitarte III (HS; de la Rúa & Hervella, 2011); 14: Alkerdi (Barandiarán & Cava, 2008); 15: Isturitz (HS; Henry-Gambier, Normand, & Pétilion, 2013); 16: Duruthy (HS; ~~Henry-Gambier, 2006~~~~Arambourou & Genet-Varein, 1965~~). N=Neandertal; HS=*Homo sapiens*. Base map made with QGIS 2.18.17 (QGIS Development Team, 2009) with data by Jarvis, Reuter, Nelson, & Guevara (2008).

**FIGURE 2** Excavation plan (a) and stratigraphic column (b) of Axlor cave (modified from Gómez-Olivencia et al., 2018a). (a) In the excavation plan the grid system used by J.M. Barandiarán (black square and white numbers) and the excavation area is shadowed in gray. The grid system used by the recent excavations is marked using black letters and numbers and the excavation area is outlined using a thick black line. The dotted line represents the rock-shelter wall when the site was first excavated, during the excavation this wall went back, revealing a possible cave infilling. The colors correspond to the levels to which these remains were attributed based on the notes by

1  
2 Barandiarán. (b) Synthetic section of the 1967–1974 excavation stratigraphy, drawn from the  
3  
4 description of the layers by J. M. Barandiarán (1980). Different levels are marked with different  
5  
6 colors, and the human remains are marked by silhouettes.  
7  
8  
9

10  
11 **FIGURE 3** Ax.11B.415.400 left parietal fragment. The original fossil and the 3D model are  
12  
13 shown on different views. On the lower row, the approximate location of this fragment is shown on  
14  
15 the La Ferrassie 1 Neandertal cranium (left), a thickness map (from 2 to 12 mm) is shown (middle)  
16  
17 with PC that correspond to thicker bone where is located the postcentral sulcus and V to a relative  
18  
19 thinning produced by the anterior ramus of the meningeal system; and the anatomical features on  
20  
21 the endocranial surface (right): including meningeal veins, A = anterior branch, O = obelisc branch,  
22  
23 and sulcal imprints C = central sulcus, PC = postcentral sulcus.  
24  
25  
26  
27  
28

29  
30 **FIGURE 4** Ectocranial view of the specimen Ax.11B.415.400 with the location of zones a-d,  
31  
32 and detailed images of these zones, where striations are located. In some cases, the grooves show a  
33  
34 close “V” shape but do not show microstriations. The general morphology of these grooves (see  
35  
36 text) make them compatible with trampling marks.  
37  
38  
39  
40

41  
42 **FIGURE 5** Dental remains previously studied by Basabe (1973) and Rostro-Carmona (2013),  
43  
44 and likely belonging to the same individual. The teeth are shown in mesial, buccal, distal, lingual  
45  
46 (top) and occlusal (bottom) views, together with the results of the enamel segmentation and the EDJ  
47  
48 surface morphology. Pulp chamber volumes (in blue) are shown in mesial ( $P^4$ ,  $M^1$ ) and lingual ( $M^2$ )  
49  
50 views. A virtual reconstruction of the teeth in buccal and occlusal views is also provided. Scale bars  
51  
52 = 1 cm.  
53  
54  
55  
56

57  
58 **FIGURE 6** Principal components analysis of shape (left column) and form variation (right  
59  
60 column), corresponding to the teeth previously studied by Basabe (1973) and Rostro-Carmona



1  
2 (2013), and likely belonging to the same individual. The Axlor remains have been compared to  
3  
4 Neandertals (NEA), fossil *Homo sapiens* (FSAP) and recent *Homo sapiens* (RSAP). In both form  
5  
6 and shape space, the Axlor remains align more closely with modern humans. TPS-grids show  
7  
8 anatomical variation corresponding to the positive and negative extreme of each PC when all the  
9  
10 other PCs are held equal to 0. For M<sup>1</sup> variation, the two data points correspond to Axlor's variation  
11  
12 before (darker red) and after (lighter red) correcting the enamel cracks ([Supplementary information](#)  
13  
14 [Figure S13](#)).  
15  
16  
17  
18  
19

20 **FIGURE 7** New dental remains from the Barandiarán collection of Axlor. AX.5B.299.16 (right  
21  
22 permanent first lower incisor, I<sub>1</sub>): root canal morphology (blue) in mesial view; mesial, buccal,  
23  
24 distal, lingual and occlusal views. AX.5B.299.31.64.17 (upper left first deciduous incisor, dI<sup>1</sup>): top,  
25  
26 mesial, buccal, distal, lingual and occlusal views. AX.9E.283.103 (left dM<sup>2</sup>): top, mesial, buccal,  
27  
28 distal, lingual and occlusal views. In the virtual reconstructions, enamel is represented in white and  
29  
30 dentine in brown. Scale bars = 1 cm  
31  
32  
33  
34  
35  
36  
37  
38  
39  
40  
41  
42  
43  
44  
45  
46  
47  
48  
49  
50  
51  
52  
53  
54  
55  
56  
57  
58  
59  
60

1  
2 The human remains from Axlor (Dima, Biscay, Northern Iberian Peninsula)  
3  
4  
5

6 Asier Gómez-Olivencia<sup>a,b,c,d\*</sup>  
7

8 Diego López-Onaindia<sup>e</sup>  
9

10 Nohemi Sala<sup>f,d</sup>  
11

12 Antoine Balzeau<sup>g,h</sup>  
13

14 Ana Pantoja-Pérez<sup>d</sup>  
15

16 Ignacio Arganda-Carreras<sup>i,b,j</sup>  
17

18 Mikel Arlegi<sup>a,k</sup>  
19

20 Joseba Rios-Garaizar<sup>f</sup>  
21

22 Aida Gómez-Robles<sup>l,m,n</sup>  
23  
24  
25  
26  
27  
28

29 <sup>a</sup>Dept. Estratigrafía y Paleontología, Facultad de Ciencia y Tecnología, Universidad del País Vasco-  
30 Euskal Herriko Unibertsitatea (UPV/EHU). Barrio Sarriena s/n, 48940 Bilbao, Spain.  
31

32 <sup>b</sup>IKERBASQUE. Basque Foundation for Science, Bilbao, Spain.  
33

34 <sup>c</sup>Sociedad de Ciencias Aranzadi, Zorroagaina 11, 20014 Donostia-San Sebastian, Spain.  
35

36 <sup>d</sup>Centro UCM-ISCIH de Investigación sobre Evolución y Comportamiento Humanos, Avda.  
37 Monforte de Lemos 5 (Pabellón 14), 28029 Madrid, Spain.  
38

39 <sup>e</sup>GREAB, Unitat d'Antropologia Biològica, Departament de Biologia Animal, Biologia Vegetal i  
40 Ecologia, Facutat de Biociències, Universitat Autònoma de Barcelona, 08193 Bellaterra, Spain.  
41

42 <sup>f</sup>Centro Nacional de Investigación sobre la Evolución Humana (CENIEH), Paseo de la Sierra de  
43 Atapuerca 3, 09002 Burgos, Spain.  
44

45 <sup>g</sup>Équipe de Paléontologie Humaine, UMR 7194, CNRS, Département Homme et Environnement,  
46 Muséum national d'Histoire naturelle. Musée de l'Homme, 17, Place du Trocadéro, 75016 Paris,  
47 France  
48

49 <sup>h</sup>Department of African Zoology, Royal Museum for Central Africa, Tervuren, Belgium  
50  
51  
52  
53  
54  
55  
56  
57  
58  
59  
60

<sup>i</sup>Dept. Ciencias de la Computacion e Inteligencia Artificial. Facultad de Informatica, Universidad del País Vasco-Euskal Herriko Unibertsitatea (UPV/EHU) Manuel Lardizabal Ibilbidea 1, 20018 Donostia, Gipuzkoa, Spain.

<sup>j</sup>Donostia International Physics Center (DIPC). Manuel Lardizabal Ibilbidea 4, 20018 Donostia, Gipuzkoa, Spain.

<sup>k</sup>Université de Bordeaux, PACEA UMR 5199, Bâtiment B8, Allée Geoffroy Saint-Hilaire, 33615 Pessac, France.

<sup>l</sup>Department of Anthropology, University College London, WC1E 0BW London, UK.

<sup>m</sup>Department of Genetics, Evolution and Environment, University College London, WC1E 6BT London, UK.

<sup>n</sup>Department of Life Sciences, Natural History Museum, SW7 5BD London, UK.

#### Correspondence

Asier Gómez-Olivencia, Dept. Estratigrafía y Paleontología, Facultad de Ciencia y Tecnología, Universidad del País Vasco-Euskal Herriko Unibertsitatea (UPV/EHU). Barrio Sarriena s/n, 48940 Bilbao, Spain.

Email: [asier.gomez@ehu.eus](mailto:asier.gomez@ehu.eus) (A.G.-O.)

## Abstract

**Objectives:** We provide the description and comparative analysis of all the human fossil remains found at Axlor during the excavations carried out by J.M. Barandiarán from 1967 to 1974: a cranial vault fragment and eight teeth, five of which likely belonged to the same individual, although two are currently lost. Our goal is to describe in detail all these human remains and discuss both their taxonomic attribution and their stratigraphic context.

**Materials and methods:** We describe external and internal anatomy, and use classic and geometric morphometrics. The teeth from Axlor are compared to Neandertals, Upper Paleolithic and recent modern humans.

**Results:** Three teeth (a left  $dm^2$ , a left  $di^1$ , and a right  $I_1$ ) and the parietal fragment show morphological features consistent with a Neanderthal classification, and were found in an undisturbed Mousterian context. The remaining three teeth (plus the two lost ones), initially classified as Neandertals, show morphological features and a general size that are more compatible with their classification as modern humans.

**Discussion:** The combined anatomical and stratigraphic study suggest that the remains of two different adult Neandertals have been recovered during the old excavations performed by Barandiarán: a left parietal fragment (level VIII) and a right  $I_1$  (level V). Additionally, two different Neanderthal children lost deciduous teeth during the formations of levels V (left  $di^1$ ) and IV (right  $dm^2$ ). In addition, a modern human individual is represented by five remains (two currently lost) from a complex stratigraphic setting. Some of the morphological features of these remains suggest that they may represent one of the scarce examples of Upper Paleolithic modern human remains in the northern Iberian Peninsula, which should be confirmed by further testing.

1  
2  
3  
4  
5  
6  
7  
8  
9  
10  
11  
12  
13  
14  
15  
16  
17  
18  
19  
20  
21  
22  
23  
24  
25  
26  
27  
28  
29  
30  
31  
32  
33  
34  
35  
36  
37  
38  
39  
40  
41  
42  
43  
44  
45  
46  
47  
48  
49  
50  
51  
52  
53  
54  
55  
56  
57  
58  
59  
60

**KEYWORDS**

Neandertal, anatomically modern humans, enamel-dentine junction, geometric morphometrics,  
Paleolithic

## 1-Introduction

The rock-shelter of Axlor is located in the mountainous region included in the national park of Urkiola (Biscay, Basque Country) and preserves one of the most important Middle Paleolithic sequences in the northern Iberian Peninsula (Figure 1). Axlor was discovered in 1932 by the Basque prehistorian J. M. Barandiarán. The first archaeological excavations took place in 1967, and encompassed a total of eight field seasons until 1974 (Barandiarán, 1980). These excavations revealed a sequence of nine layers (I-IX), in which Middle Paleolithic lithic assemblages were found in levels III to VIII. Recent excavations (2000-2008) directed by González-Urquijo, Ibáñez and Rios-Garaizar, provide a new stratigraphic sequence, roughly equivalent to the previous one, but with additional levels, not previously identified or excavated by Barandiarán. Some of these levels were deposited before level VIII, but their chronology remains uncertain (González-Urquijo, Ibáñez, Lazuén & Mozota, 2014; Rios-Garaizar, 2017). Additionally, an early Upper Paleolithic occupation has been recognized (level A of the new excavations, equivalent to the base of Barandiarán's level II, previously considered sterile; González-Urquijo et al., 2014). Ultra-filtered dates obtained from red deer with anthropogenic marks from level IV have yielded results that go beyond the radiocarbon limit, correcting previous dating which situated this level at the very end of regional Middle Paleolithic (Marín-Arroyo et al., 2018). Across the sequence, there are clear differences in terms of the technological characteristics, percentage of ungulate taxa consumed, and type of occupation of the cave between the upper (III-VI) and lower levels (VII-VIII) of the Mousterian sequence, which has been confirmed during the recent excavations (Altuna, 1989; Castaños, 2005; González-Urquijo et al., 2014; Rios-Garaizar, 2017). Recent reassessment of the Barandiarán collection has identified the presence of bird and carnivore exploitation for the first time during the Middle Paleolithic of the Cantabrian region: at least a golden eagle and a lynx where exploited for dietary purposes (Gómez-Olivencia et al., 2018a).

1  
2 [INSERT FIGURE 1 HERE]  
3  
4  
5  
6

7 The current human fossil record published for Axlor is limited to five upper left dental  
8 remains (C, P<sup>4</sup>-M<sup>3</sup>) with a maxilla fragment, likely belonging to the same individual (a young  
9 adult), which were found in 1967 from a level with Quina Mousterian lithics and faunal remains of  
10 red deer, reindeer, and steppe bison (Basabe, 1973; [Figure 2](#)). Basabe (1973) seems to be cautious  
11 in the taxonomic assessment of these remains. While he considers that the morphology of these  
12 dental remains is compatible with that found in similar (Mousterian) archaeological contexts, he  
13 nonetheless considers these remains as “evolved”, with “intermediate” size and traits, including the  
14 “unclear” taurodontism in M1-M2 (Basabe, 1973). Currently, only three (P<sup>4</sup>, M<sup>1</sup>, M<sup>3</sup>) of these  
15 remains are curated at the Arkeologi Museoa (Bilbao), whereas the location of the other teeth is  
16 unknown. A more recent reassessment of these teeth supported a Neandertal classification based on  
17 their size and the alleged presence of taurodontism in the molars (Rostro-Carmona, 2013).  
18 However, a visual inspection of the morphology of the M<sup>1</sup> shows that it does not present the typical  
19 Neandertal morphology for this tooth (e.g., Bailey, 2004; Gómez-Robles et al., 2007). Moreover, no  
20 study of the internal anatomy of the teeth based on virtual anthropology techniques has been  
21 performed, which could provide a more accurate taxonomic assessment. In 2005, the re-assessment  
22 of the whole Barandiarán collection (coordinated by J.E. González Urquijo) resulted in the  
23 recognition of three additional human remains: two teeth and a cranial fragment. More recently, the  
24 reassessment of the faunal collection from Barandiarán's excavation has resulted in the  
25 identification of an additional human remain among the faunal remains: an upper deciduous molar.  
26  
27  
28  
29  
30  
31  
32  
33  
34  
35  
36  
37  
38  
39  
40  
41  
42  
43  
44  
45  
46  
47  
48  
49  
50  
51  
52

53 [INSERT FIGURE 2 HERE]  
54  
55  
56

57 Here we provide a detailed description and comparative analysis of all the human fossil  
58 remains from Axlor found during J.M. Barandiarán's excavations, including a taphonomic analysis  
59  
60

1  
2 of the cranial fragment. This study also reassess the taxonomic affinities of the remains published  
3  
4 by Basabe (1973) and Rostro-Carmona (2013), and discusses the archaeological context of all the  
5  
6 human remains from this collection. In fact, the revision of the archaeological context from the  
7  
8 field-notes taken by J.M. de Barandiarán at the site casts doubts on the stratigraphic position of all  
9  
10 the teeth studied by Basabe (1973) and Rostro-Carmona (2013), while in the rest of the cases the  
11  
12 association of these human remains to Mousterian contexts seems secure ([Supplementary](#)  
13  
14 [Information Text S1](#)).  
15  
16  
17  
18  
19  
20  
21

## 22 **2-Materials and Methods**

### 23 *2.1-Materials*

24  
25  
26  
27  
28  
29  
30 The current collection of human remains from the Barandiarán excavations includes an  
31  
32 upper fourth premolar, an upper first molar and an upper third molar from the same (young adult)  
33  
34 individual (Basabe, 1973), a cranial fragment, a lower right central incisor, an upper left first  
35  
36 deciduous incisor and a left upper deciduous second molar ([Table 1](#)). Their spatial location,  
37  
38 according to the available information is shown in [Figure 2](#). Access to these materials was granted  
39  
40 by the Arkeologi Museoa (Bilbao). The CT scans of these fossils, the derived segmentation files,  
41  
42 and 3D volumes are freely accessible.  
43  
44  
45  
46  
47

48 [INSERT TABLE 1 HERE]  
49  
50  
51  
52  
53

### 54 *2.2-Micro-CT scanning*

55  
56  
57 All the Axlor human remains were micro-CT scanned at the Spanish National Research  
58  
59 Center for Human Evolution (CENIEH) using a Phoenix v/tome/x s (GE Measurement & Control).  
60



1  
2 The resolution was maximized depending on the size of the different fossil remains (teeth:  
3  
4 18.99 $\mu\text{m}$ ; cranial fragment: 33 $\mu\text{m}$ ).  
5  
6  
7  
8

### 9 *2.3-Anatomical descriptions*

10  
11 Standard methods were used to describe and analyze the external and internal anatomy of  
12  
13 the cranial fragment. Previous knowledge of the anatomy and relative variation of exo and  
14  
15 endocranial surfaces was used to identify the anatomical position and diagnostic features of the  
16  
17 cranial fragment (e.g., Balzeau, 2013; Balzeau, Grimaud-Hervé & Gilissen, 2011; Balzeau et al.,  
18  
19 2017). The teeth were described following established anatomical dental terms (Carlsen, 1987). In  
20  
21 addition, we scored several non-metric traits following both the Arizona State University Dental  
22  
23 Anthropology System (ASUDAS) (Turner, Nichol & Scott, 1991) and some complementary traits  
24  
25 described by Bailey (2002), which were compared to Neandertals, Upper Paleolithic modern  
26  
27 humans (UPMH) and recent humans (Martinón-Torres, Bermúdez de Castro, Gómez-Robles,  
28  
29 Prado-Simón, & Arsuaga, 2012). Some of these traits were also scored in the EDJ surface and  
30  
31 completed by the traits described by Martin, Hublin, Gunz, & Skinner (2017) for the molars. The  
32  
33 roots of the incisors were measured following the method described by Le Cabec, Gunz, Kupczik,  
34  
35 Braga & Hublin (2013): Root Length (RL), Root Volume (RV), Root Pulp Volume (RPV), Crown  
36  
37 Pulp Volume (CrPV) and different ratios between these measurements. Dental wear assessment was  
38  
39 based on Molnar (1971).  
40  
41  
42  
43  
44  
45  
46  
47

### 48 *2.4-Bone thickness mapping (cranial fragment) and volume segmentation (teeth)*

49  
50 The 3D variation of the total bone thickness of the cranial fragment was evaluated using the  
51  
52 exo- and endocranial surfaces using the module Surface-Distance of Avizo 7. The results of this  
53  
54 analysis were illustrated using a chromatic scale and compared to previous studies (Balzeau, 2013)  
55  
56 in order to gain insights on the potential taxonomic significance of the thickness distribution  
57  
58 pattern.  
59  
60

1  
2 In the case of the teeth, before their segmentation, the CT image volumes were pre-  
3  
4 processed using Fiji (Schindelin et al., 2012) by first converting them to 8-bit and then re-sampling  
5  
6 them in the Z direction by a factor of 2 (final volume resolution: 0.019 x 0.019 x 0.038 microns per  
7  
8 voxel). Next, the volumes were segmented using an interactive learning approach (Arganda-  
9  
10 Carreras et al., 2017) that classified each voxel as belonging to one of the following classes: bone,  
11  
12 dentine, enamel, or background. The pulp chamber was afterwards labeled by semi-automatic  
13  
14 filling of the cavity inside the other teeth labels. The output label images were cleaned up by  
15  
16 removing small artifacts and noise by means of morphological operations (Legland, Arganda-  
17  
18 Carreras & Andrey, 2016). Finally, we performed manual correction of the segmented images using  
19  
20 AvizoLite software due to the presence of cracks in some teeth, and lower density zones in the  
21  
22 enamel some of the teeth.  
23  
24  
25  
26  
27  
28

### 29 *2.5-Taphonomic analysis*

31  
32 The cranial bone was macroscopically and microscopically examined using a hand lens and a  
33  
34 stereoscopic zoom microscope (Olympus SZX10) to examine surface modifications. For the  
35  
36 analysis of striae regarding the differentiation between cut marks and trampling marks we have used  
37  
38 the protocol proposed by Domínguez-Rodrigo, de Juana, Galán & Rodríguez (2009). The cranial  
39  
40 breakage pattern was analyzed following the criteria developed by Sala, Pantoja-Pérez, Arsuaga,  
41  
42 Pablos & Martínez (2016) to assess the presence/absence of perimortem (fresh bone) and  
43  
44 postmortem (dry bone) fractures. Four parameters were recorded: fracture outline (linear, depressed,  
45  
46 stellate); fracture angle (right or oblique); fracture edge (smooth or jagged); presence/absence of  
47  
48 cortical delamination.  
49  
50  
51  
52  
53

### 54 *2.6-Geometric morphometrics*

55  
56  
57 Geometric morphometric analyses of the occlusal surface of the premolar and molar crowns  
58  
59 were used to compare the Axlor posterior permanent teeth with the Neandertal and modern human  
60

1  
2 samples used in Gomez-Robles et al. (2007), Gómez-Robles, Bermúdez de Castro, Martín-  
3  
4 Torres, Prado-Simón, & Arsuaga (2012), and Gómez-Robles, Martín-Torres, Bermúdez de  
5  
6 Castro, Prado-Simón, & Arsuaga (2011). Modern human samples included both fossil and recent  
7  
8 modern humans. Occlusal photographs were used to place 2D configurations of landmarks and  
9  
10 semilandmarks. For the M<sup>1</sup>, analyses were repeated on the original photographs and on an occlusal  
11  
12 projection of the occlusal surface obtained after virtually correcting enamel cracks. Because the  
13  
14 Axlor M<sup>1</sup> is heavily worn, the location of anatomical landmarks on cusp apices cannot be  
15  
16 unequivocally determined. Therefore, M<sup>1</sup> analyses were repeated twice, using the original  
17  
18 configuration of landmarks and semilandmarks as described in Gómez-Robles et al. (2007) and only  
19  
20 the configuration of outline semilandmarks (after removing the four anatomical landmarks). The  
21  
22 second analysis, therefore, focuses on the ability of the M<sup>1</sup> occlusal outline to differentiate  
23  
24 Neandertal from modern human molars. The Axlor P<sup>4</sup> and M<sup>3</sup> are substantially less worn than the  
25  
26 M<sup>1</sup>, so only the complete configuration of landmarks and semilandmarks was evaluated for them.  
27  
28 For all the posterior teeth, geometric morphometric analyses were performed that included and  
29  
30 excluded size variation (in form and shape space, respectively). A discriminant analysis based on  
31  
32 the first ten principal components of shape variation was carried out to evaluate the species that  
33  
34 Axlor teeth are assigned to.  
35  
36  
37  
38  
39  
40  
41  
42  
43  
44

### 45 **3-Metric, morphological and taphonomic description**

46  
47  
48  
49

50 The cranial and the dental remains are described here. The comparison of the external crown  
51  
52 metric data between Axlor teeth and different comparative samples are shown in [Table 2](#). Only  
53  
54 taxonomically useful metric traits are discussed below.  
55  
56  
57  
58

59 [INSERT TABLE 2 HERE]  
60

### 3.1-Cranial fragment

AX.11B.415.400 is a fragment (56 × 41 mm) of a left parietal bone, which preserves 54 mm of the sagittal suture (Figure 3). The suture is not fused, and this left fragment has been separated from the right parietal bone without any breakage of the indentations. Bone thickness for the analyzed area is only slightly smaller than in La Ferrassie 1 (Balzeau, 2013) and thus incompatible with a young immature status. Thus, the fragment is not from a child, but may belong to a young adult or adult. The antero-posterior curvature of this fragment is not very pronounced.

[INSERT FIGURE 3 HERE]

Bone thickness distribution was quantified on nearly the whole preserved area of this fragment. Thickness varies between 3.4 mm and 10.5 mm. The mean thickness of the fragment is 5.4 mm. Thickness is evenly distributed along the surface of the fragment, there is no clear increase or decrease related to bone thickness variation. The only exception concerns the blood vessels on the endocranial surface of the anterior border of the fragment, which are associated with a clear thinning of the bone (the area with white dots at the anterior border of the bone, noted V on Figure 3). Moreover, the infero-anterior corner of the fragment shows a slight increase in bone thickness (represented by the purple area, noted PC on Figure 3) which continues posteriorly and obliquely. It corresponds to the postcentral sulcus.

Some clear endocranial features are visible. Some branches of the meningeal system are noticeable. They probably all belong to the anterior ramus, one being the anterior branch (noted A on Figure 3), the second corresponding to the obelic branch (noted O on Fig. 3). The anterior branch splits in two simple veins that are quite large. The obelic branch splits into two smaller and long veins. Concerning the gyral pattern visible on this endocranial surface, two sulci are clear. The

1  
2 course of the postcentral sulcus (noted PC on [Figure 3](#)) goes from the antero-inferior corner of the  
3  
4 fragment to the center of the medial border of the fragment. This sulcus is well printed and shows a  
5  
6 clear course. Anteriorly, the central sulcus (noted C on [Figure 3](#)) seems to run along the course of  
7  
8 the most anterior vein of the anterior ramus. Those two sulci have a parallel course, delimiting a  
9  
10 post-central gyrus that has a regular width on its preserved extension.  
11  
12  
13  
14  
15

16 Both bone thickness distribution pattern and endocranial anatomy provide information that  
17  
18 helps to propose a taxonomic attribution for this fragment. Bone thickness shows little variation. In  
19  
20 modern humans, there is a clear decrease in bone thickness in the area of the superior parietal gyrus.  
21  
22 The pattern observed on this fragment resembles what has been described for Neandertals (Balzeau,  
23  
24 2013). The position and size of the anterior branch of the meningeal system on this fragment, as  
25  
26 well as its subsequent bone thickness variation, fits with the anatomy observed in Neandertals. The  
27  
28 meningeal system in this area has more anastomoses than in modern humans, and blood vessels are  
29  
30 thinner and more numerous (Grimaud-Hervé, 1997). In summary the anatomical features preserved  
31  
32 in this parietal fragment are consistent with a Neandertal classification.  
33  
34  
35  
36  
37  
38

39 The bone surface of the cranial fragment is well preserved and does not show weathering  
40  
41 (sensu Behrensmeyer, 1978). No direct carnivore activity (i.e., tooth marks) was documented, nor  
42  
43 any sign of burning. Similarly, no other biological modifications, such as rodent activity or root  
44  
45 etching, was observed. This cranial fragment shows several striations in the outer table in five  
46  
47 different areas ([Figure 4](#)). In some cases, the grooves are close “V” shaped, but microstriations were  
48  
49 not evident. On the other hand, the trajectories of the grooves are usually sinuous and most of the  
50  
51 bone surface is covered by very shallow striae. In some cases, the color of the striations is lighter  
52  
53 compared with the bone surface suggesting that they have occurred after its deposition. These  
54  
55 observations are compatible with trampling marks following the protocol described by Domínguez-  
56  
57 Rodrigo et al. (2009). Regarding the fracture analysis, this remain displays three linear fractures,  
58  
59  
60

1  
2 one of them parallel and two perpendicular to the cranial suture. The two fractures perpendicular to  
3  
4 the suture have right angled edges, jagged surfaces and absence of cortical delamination. These  
5  
6 characteristics are typical of fracturing in dry bone (Sala et al., 2016). However, the fracture that is  
7  
8 parallel to the suture displays an oblique angle, smooth surface and presence of cortical  
9  
10 delamination (0.75 cm) on the inner table. The combination of these fracture attributes is usually  
11  
12 considered representative of perimortem fractures (Sala et al., 2016).  
13  
14  
15  
16  
17

18 [INSERT FIGURE 4 HERE]  
19  
20  
21  
22

23 *3.2-Upper left fourth premolar, maxillary fragment with upper first molar and upper third molar*  
24  
25 *belonging to the same individual*  
26  
27  
28  
29

30 Descriptions and analyses are provided for the three dental remains belonging to the same  
31  
32 individual. These remains are shown in Figure 5 and are morphologically compared in Tables 3-5.  
33  
34  
35

36 Ax.13F.265.1 (AX.13E/13F.265-270.1 according to the museum records) is a complete  
37  
38 premolar, although its root is damaged and presents longitudinal cracks on both sides and some  
39  
40 smaller transversal cracks. In addition, there is a small pitting on the vestibular side of the buccal  
41  
42 cusp, and erosion on the tip of this cusp (Figure 5). Also, in the areas with the highest enamel  
43  
44 thickness of the crown (the buccal and lingual sides) there is a part of the enamel that shows lower  
45  
46 density in the CT images (Supplementary information Figure S12). The similarity in height between  
47  
48 the lingual and buccal cusps and the two long inter-proximal facets suggest it is a P<sup>4</sup>. In addition,  
49  
50 the distal interproximal wear facet matches well the mesial counterpart of the Axlor M<sup>1</sup> (Figure 5),  
51  
52 further supporting that this is a P<sup>4</sup>, and indicating that they both belonged to the same individual  
53  
54  
55  
56  
57 (see below).  
58  
59  
60

1  
2 [INSERT FIGURE 5 HERE]  
3  
4  
5

6 The occlusal surface is moderately worn (stage 3; Molnar, 1971), and the dentine is exposed  
7 on the lingual cusp. Yet, the inter-proximal wear facets are visible to the naked eye, and the distal  
8 one is larger. This premolar shows a distal accessory marginal tubercle, a bifurcated buccal essential  
9 crest (grade 2 from Bailey, 2002) and a distal accessory ridge on the buccal cusp (Table 3).  
10  
11  
12  
13  
14  
15  
16  
17

18 [INSERT TABLE 3 HERE]  
19  
20  
21  
22

23 At the EDJ level, two major cusps are observed: buccal and lingual. The essential crest of  
24 both the lingual and buccal cusps are bifurcated (Grade 2; Table 3), which are features typically  
25 observed on Neandertals (92.3% and 61.5% respectively). On the mesial side it presents a  
26 continuous transverse crest that does not connect with the horn tip of the lingual cusp, also typical  
27 in Neandertals (69.2%). In addition, there is an intermediate accessory marginal tubercle distal to  
28 the buccal cusp. The coronal pulp cavity is conformed by the two horns corresponding to the main  
29 cusps, where the buccal horn is almost two times larger than the lingual one.  
30  
31  
32  
33  
34  
35  
36  
37  
38  
39  
40

41 This premolar shows a single, mediolaterally flat root. This root runs wide and straight in  
42 the most cervical half, while the apical third is narrower. Both the mesial and distal sides present  
43 longitudinal grooves, of which the distal is more pronounced. The analysis of the root canal based  
44 on the  $\mu$ CT images shows that this is a single canal (Type 1R<sub>1</sub>) which is only found in 12.5% of  
45 Neandertals (Pan & Zanolli, 2019; Table 3).  
46  
47  
48  
49  
50  
51  
52  
53  
54

55 Geometric morphometric analyses show that Neandertals and recent modern humans are  
56 almost completely separated along the P<sup>4</sup> morphospace, with Neandertals showing a lingually  
57 expanded and asymmetric morphology and modern humans showing a symmetric and lingually  
58  
59  
60

1  
2 reduced configuration, where the interfoveal distance is strongly reduced (Figure 6; Gómez-Robles  
3  
4 et al., 2011). Interestingly, fossil modern humans completely overlap with Neandertals, showing a  
5  
6 premolar configuration that is much more similar to that of Neandertals than to that of recent  
7  
8 modern humans. The Axlor P<sup>4</sup> plots right on the imaginary line that separates the areas of  
9  
10 distribution of Neandertals and recent modern humans, but outside the range of distribution of both  
11  
12 groups. The Axlor P<sup>4</sup> plots on this intermediate position because it shares a generally asymmetric  
13  
14 morphology with Neandertals, but a moderately reduced distal cusp and a shortened interfoveal  
15  
16 distance with modern humans. Based on these traits, a discriminant analysis classifies the Axlor P<sup>4</sup>  
17  
18 as a modern human, but with a low probability of only 56%. When adding size information, the  
19  
20 Axlor P<sup>4</sup> plots again in an intermediate position between Neandertals and recent modern humans.  
21  
22 Interestingly, it also plots on the lower extreme of the size variation found in fossil modern humans,  
23  
24 indicating that the Axlor P<sup>4</sup> is larger than most recent modern humans, but smaller than most  
25  
26 Neandertals and fossil modern humans.  
27  
28  
29  
30  
31  
32  
33

34 [INSERT FIGURE 6 HERE]  
35  
36  
37  
38  
39  
40

41 Ax.13F.265.3 (AX.13E/13F.265-270.3 according to the museum records) represents a left  
42  
43 maxilla fragment, preserving both the external surface (ca. 13.3 × 9.2 mm), and the internal surface  
44  
45 (13.4 × 9.8 mm), with the left M<sup>1</sup> placed in its alveolus. This tooth is fragmented due to longitudinal  
46  
47 and transversal cracks that affect the crown and roots (Figure 5). Inter-proximal wear facets are  
48  
49 clear in both sides and the mesial one shows clear grooves on it. This mesial facet shows two  
50  
51 chippings in its occlusal border. Also, the occlusal surface of the tooth is heavily worn (stage 4-5;  
52  
53 Molnar, 1971) and the dentine is exposed in all four main cusps, which interferes with the  
54  
55 observation of several morphological traits.  
56  
57  
58  
59  
60



1  
2 The metacone and the hypocone of this molar are well developed (grade 4 ASUDAS), and  
3  
4 there is no cusp 5 (Table 4). The hypocone is not distolingually projected, but it is aligned with the  
5  
6 protocone on the lingual side and with the metacone on the distal side. Due to the heavy occlusal  
7  
8 wear, it is not possible to score the presence of Carabelli's tubercle or the mesial marginal accessory  
9  
10 tubercle. The EDJ reveals the presence of an intermediate post-paracone tubercle and no sign of  
11  
12 fifth cusp (Table 4). Moreover, there is a type II *crista obliqua*, continuously connecting the  
13  
14 metacone to the protocone, which is centrally positioned. The occlusal wear also affects the dentine  
15  
16 to a large extent, which may influence trait assessments, but a Carabelli's tubercle does not seem to  
17  
18 be present. The horn tip of the hypocone pulp cavity is small and not projected, in contrast with the  
19  
20 typical Neandertal morphology (Supplementary Information Figure S14).  
21  
22  
23  
24  
25  
26

27 [INSERT TABLE 4 HERE]  
28  
29  
30  
31

32 The three roots are separated, all the radicular canals are divergent and the body is relatively  
33  
34 short. The canal corresponding to the mesio-buccal root is the widest one, being mesiodistally flat.  
35  
36 Moreover, the cervical third of this root canal is elongated, presenting a wide morphology, and the  
37  
38 apical end is bifurcated. This root morphology contrasts with the typical Neandertal taurodont  
39  
40 configuration.  
41  
42  
43  
44

45 Analyses of shape variation show a generally clear separation between Neandertals and  
46  
47 modern humans, with Neandertals showing a skewed M<sup>1</sup> configuration and modern humans  
48  
49 showing a squared configuration (Figure 6; Bailey, 2004; Gómez-Robles et al., 2007). Both groups  
50  
51 show a minor overlapping area where many fossil modern humans, as well as the Axlor M<sup>1</sup>, are  
52  
53 found. Based on shape data, Axlor M<sup>1</sup> is classified as a modern human with a probability of 88.8%  
54  
55 or 98.6% (before and after correcting the enamel cracks, respectively). Because of the small size of  
56  
57  
58  
59  
60

1  
2 the Axlor M<sup>1</sup>, adding size information to the PCA makes this specimen plot comfortably within the  
3  
4 modern human range of distribution.  
5  
6  
7

8  
9 When assessing only the M<sup>1</sup> outline as defined by curve semilandmarks ([Supplementary](#)  
10  
11 [Information Figure S15](#)), the differentiation between Neandertals and modern humans is less clear.  
12  
13 There is still an area of the morphospace occupied only for Neandertals and another one occupied  
14  
15 only by modern humans on the grounds of their skewed or squared outline configurations,  
16  
17 respectively. However, the overlapping area between both species is larger in this case.  
18  
19 Irrespectively of whether enamel cracks are corrected or not, the Axlor M<sup>1</sup> plots again in the area of  
20  
21 overlapping of both species. Outline shape data also classify the Axlor M<sup>1</sup> as a modern human with  
22  
23 a very high probability of more than 99% (with and without enamel crack corrections). Form  
24  
25 analyses (including size information) also make Axlor M<sup>1</sup> plot comfortably within the range of  
26  
27 variation of modern humans.  
28  
29  
30  
31  
32  
33  
34  
35

36 Ax.13F.265.2 (AX.13E/13F.265-270.2 according to museum records) This tooth is well  
37  
38 preserved upper left M<sup>3</sup>. The crown is complete, but the lingual root is broken, and it is possible to  
39  
40 observe longitudinal cracks on both sides of the preserved root fragment. In addition, it shows  
41  
42 moderate wear on the buccal cusp tips but there is no exposed dentine on them (stage 2; Molnar,  
43  
44 1971).  
45  
46  
47  
48  
49

50 There is a well-developed metacone but the hypocone is absent ([Table 5](#)). Nevertheless,  
51  
52 there is a small fifth cusp, that is positioned distally to a lingual tubercle. On the EDJ it can be  
53  
54 observed that there is no crista obliqua, and that the post-paracone tubercle is intermediate ([Table](#)  
55  
56 [5](#)). Dentine horn tips of the major cusps are not centrally compressed. The preserved part of the root  
57  
58 corresponds to the two buccal roots, with both apical tips completely closed. These two roots are  
59  
60

1 fused, but the root canals run independently along most of the root, except in the most apical tip  
2  
3  
4 where they meet again.  
5  
6  
7

8  
9 [INSERT TABLE 5 HERE]  
10  
11  
12

13 Shape analyses show that the separation between Neandertal and modern human M<sup>3</sup>s is far  
14 from clear (Figure 6; Gómez-Robles et al., 2012). Both species overlap completely along PC1, and  
15 they show certain morphological trends only along PC2, with Neandertals tending to show positive  
16 values associated with a more expanded hypocone, and modern humans tending to show negative  
17 values associated with a strongly reduced hypocone that may be absent altogether. As with the other  
18 adult posterior teeth, the M<sup>3</sup> from Axlor plots on the area of the morphospace where Neandertals  
19 and modern humans overlap. Shape data classify this M<sup>3</sup> as a modern human with a probability of  
20 78.4%, but it should be noted that the percentage of correct classification for Neandertals is very  
21 low. The inclusion of size information makes this molar plot far outside the range of variation of  
22 Neandertals on the grounds of its small size.  
23  
24  
25  
26  
27  
28  
29  
30  
31  
32  
33  
34  
35  
36  
37

38 In summary, based on both morphological and size characteristics, this individual shows  
39 stronger affinities with modern humans than with Neandertals.  
40  
41  
42  
43  
44  
45  
46  
47

### 48 *3.3-Additional dental remains*

49  
50  
51

52 AX.5B.299.16 This is a well-preserved lower right first incisor, although it shows heavy wear on  
53 the incisal edge, having lost between the 20-50% of the crown (roughly equivalent to Grade 4;  
54 Molnar, 1971; Figure 7). The degree of shoveling, labial convexity and the interproximal facets  
55 cannot be assessed due to the heavy incisal wear. The bucco-lingual diameter (7.7 mm) is larger  
56  
57  
58  
59  
60

1  
2 than the one observed in modern humans and it fits well within the Neandertal range of variation. In  
3  
4 contrast, the mesio-distal diameter is slightly smaller than the Neandertal minimum and falls within  
5  
6 the modern human distribution (Table 2). Nonetheless, this mesio-distal measure is most probably  
7  
8 affected by the wear of the crown. The cingular region is bulky, although there is no tuberculum  
9  
10 dentale. The heavy wear also affects the observation of the degree of shoveling at the EDJ level,  
11  
12 where no tuberculum dentale is observed. The root length of this incisor is 20.86 mm, equal to the  
13  
14 maximum value reported in Neandertals (13.8-20.86 mm), and longer than the currently known  
15  
16 values for Upper Palaeolithic (11.84-14.20 mm) and recent modern humans (13.18-19.22 mm)  
17  
18 (comparative samples from Le Cabec et al., 2013). In addition, the root volume is higher than any  
19  
20 reported value for Neandertals or anatomically modern humans (458.33 mm<sup>3</sup>). On the other hand,  
21  
22 the volume of the crown pulp (CrPV) and the radicular canal (RpV) are in the low end of the  
23  
24 variability of Neandertals, 6.61 mm<sup>3</sup> and 2.65 mm<sup>3</sup>, respectively. The ratio between the volume of  
25  
26 these two values is 0.4, which is situated in the highest half of the Neandertal variability, indicating  
27  
28 a proportionally bigger crown pulp segment compared to the root (comparative samples from Le  
29  
30 Cabec et al., 2013). In sum, the features observed on this tooth (in particular, its crown and root  
31  
32 length size) align it with Neandertals.  
33  
34  
35  
36  
37  
38  
39  
40

41 [INSERT FIGURE 7 HERE]  
42  
43  
44

45 AX.5B.299.31.64.17 This is an upper left first deciduous incisor with a well-preserved crown, but  
46  
47 the root is not complete (Figure 7). The smooth and twisted aspect of the fracture line of the root  
48  
49 has been interpreted in other individuals as the result of root resorption, corresponding to a 6-8-  
50  
51 years-old individual based on modern standards (AlQahtani, Hector, & Liversidge, 2010). Despite  
52  
53 the heavy wear (Grade 5, Molnar, 1971), a marked shovel shape is observable on the enamel  
54  
55 surface (>3 ASUDAS). The mesio-distal diameter of this incisor falls within the metric variation of  
56  
57 both Neandertals and modern humans, but the bucco-lingual diameter is larger than the maximum  
58  
59  
60

1  
2 value for the latter group (Table 2). There is no tuberculum dentale, and it is not possible to evaluate  
3  
4 the labial convexity on the enamel. The EDJ shows a strong and asymmetric labial convexity, more  
5  
6 marked on the mesial side than on the distal. Moreover, there is no tuberculum dentale observed at  
7  
8 the EDJ level, and it shows a well-developed shovel shape (>3 ASUDAS). In sum, the features  
9  
10 observed on this tooth (in particular, its strong and asymmetric labial convexity, its well-developed  
11  
12 shovel shape) and its size align it with Neandertals.  
13  
14  
15  
16  
17  
18  
19

20 AX.9E.283.103 This tooth is an upper left second deciduous molar that preserves a nearly complete  
21  
22 crown. The tooth is heavily worn exhibiting dentine in all four cusps, and the mesial inter-proximal  
23  
24 side of the enamel is missing. This tooth does not preserve the root, likely resorpted and/or  
25  
26 subsequently broken, and would have belonged to a 10-11-years-old individual based on modern  
27  
28 standards (AlQahtani et al., 2010). The size of the crown of this specimen does not provide  
29  
30 taxonomic information due to the large overlap between Neandertals and modern humans (Table 2).  
31  
32 Both the metacone and the hypocone are well developed (grade 4 ASUDAS). Despite the heavy  
33  
34 wear, it is possible to observe a big Carabelli's trait (Grade > 2 ASUDAS), but it is not possible to  
35  
36 assess the presence of any other accessory tubercles. The EDJ presents a big Carabelli's trait that is  
37  
38 affected by the fracture of the mesial interproximal side of the tooth, which does not allow locating  
39  
40 the dentine horn. Moreover, the crista obliqua is continuous, and of type II, with a centered placed  
41  
42 protocone, which is a typical Neandertal trait (Becam et al., 2015; Becam & Chevalier, 2019). A  
43  
44 quantitative analysis of this molar has not been carried out, but qualitative observation shows that  
45  
46 the skewed morphology typical of Neandertal dm<sup>2</sup>s is not present (Bailey et al., 2014). A generally  
47  
48 squared outline morphology is present in this specimen instead. This squared morphology may  
49  
50 result from the presence of a well-developed Carabelli's trait, which is reported to give Neandertal  
51  
52 dm<sup>2</sup>s a less skewed appearance (Bailey et al., 2014). In sum, most features observed on this tooth  
53  
54 align it with Neandertals.  
55  
56  
57  
58  
59  
60

## Discussion

### *Taxonomic assessment of the Axlør fossil remains*

The human remains from Axlør can be divided into two different groups. The first group includes a series of published dental remains, traditionally regarded as belonging to a single Neandertal individual (Basabe, 1973), which our results better classify as belonging to a modern human. Indeed, a detailed evaluation of the field notes of J.M. Barandiarán and our own assessment of the stratigraphy at the place where these remains were found cast doubts regarding their belonging to the Middle Paleolithic layers ([Supplementary Information Text S1](#)). The second group of human remains includes three dental remains and a cranial fragment, described here for the first time, which show clear Neandertal affinities and whose attribution to Mousterian layers seems secure based on our assessment of the J.M. Barandiarán field notes.

The first group includes three teeth, P<sup>4</sup>, M<sup>1</sup> and M<sup>3</sup> (plus two additional lost specimens), likely belonging to the same individual as already stated by Basabe (1973). The (moderate) wear stage and the fact that the apical tip of the M<sup>3</sup> root is closed indicates that they belonged to a young adult. Several features, mainly related to the M<sup>1</sup> morphology, question the previous taxonomic assignment of these teeth. First, the hypocone of the M<sup>1</sup> is not bulky and projected disto-lingually ([Figures 5-6; Supplementary Information Figures S14-S15](#)), the tips of the dentine horns, as far as it can be inferred given the heavy wear of the molar, are not centrally placed, and the molar is not taurodont. In summary, this molar lacks all the traits that are typically associated with Neandertal M<sup>1</sup>s. Second, the P<sup>4</sup> shows a single root channel (an infrequent trait in Neandertals; Pan & Zanolli, 2019), a reduced lingual cusp and a shortened interfoveal distance (typically observed in modern humans). However, other traits in this individual seem to be more frequent in Neandertals. First, the

1  
2 bifurcated buccal and lingual essential crests on the P<sup>4</sup> EDJ and the continuous transverse crest are  
3  
4 typically Neandertal features (Becam et al., 2019), as it is a generally asymmetric P<sup>4</sup> crown  
5  
6 (Gómez-Robles et al., 2011). Second, the presence of crista obliqua is a Neandertal M<sup>3</sup> common  
7  
8 feature (Martin et al., 2017), but the Axlör specimen does not present it in any typology. Moreover,  
9  
10 in this M<sup>3</sup> only the metacone dentine horn tip is slightly centrally placed, while the rest of the cusps  
11  
12 show the typical morphology of *Homo sapiens*. However, it should be noted that variation of  
13  
14 UPMH in many of these traits is not completely understood (e.g., for the P<sup>4</sup>, there is only  
15  
16 information from one UPMH; Becam et al., 2019). Moreover, the discovery of UPMH with  
17  
18 evidence of recent Neandertal admixture (Fu et al., 2015) and the mounting evidence that  
19  
20 Neandertal-modern human hybridization may have been common could partially explain the  
21  
22 differences found between the dental morphology of the UPMH and Holocene populations.  
23  
24  
25  
26  
27  
28  
29

30 In addition, a qualitative assessment of the teeth that are now lost from the collection (C\*  
31  
32 and M<sup>2</sup>), based on the information and figures provided by Basabe (1973), indicates that they likely  
33  
34 belonged to the same individual due to the overall morphology and wear degree compatibility.  
35  
36 Moreover, the M<sup>3</sup> presents a small interproximal facet, compatible with the M<sup>2</sup> with reduced  
37  
38 hypocone presented by Basabe (1973). Regarding the morphology of these two lost teeth, it is  
39  
40 possible to observe on the original publication that the upper canine has some archaic features: a  
41  
42 bulky tuberculum linguale (ASUDAS grade >3) and well developed mesial ridge (grade 2), more  
43  
44 common in Neandertals (100% and 42.1%, respectively) and UPMHs (40% and 11.1%,  
45  
46 respectively) than in recent *Homo sapiens* (8% and 5.3%, respectively) (Martinón-Torres et al.,  
47  
48 2012). On the other hand, the M<sup>2</sup> presents a large metacone (ASUDAS grade 3-4), a reduced  
49  
50 hypocone (ASUDAS grade 0-2), and absence of Carabelli's tubercle (ASUDAS grades 0-1).  
51  
52 Reduced hypocones are more common in UPMHs (50%) than in Neandertals (24.9%) (Martinón-  
53  
54 Torres et al., 2012).  
55  
56  
57  
58  
59  
60

1  
2 Based on this morphological information, the absence of Holocene recent prehistory remains  
3  
4 from the Axlor sequence, the presence of an early Upper Paleolithic occupation in the site  
5  
6 (González-Urquijo et al., 2014), and the unclear previous ascription to the Mousterian level III due  
7  
8 to their finding in loose sediment close to the rock-shelter wall (see [Supplementary information](#)),  
9  
10 we hypothesize that these human remains could belong to an UPMH, which should be tested in the  
11  
12 near future using direct C14 datings. Currently, except for a few skeletons (Lagar Velho, Mirón;  
13  
14 Duarte et al., 1999; Carretero et al., 2015) most of the Upper Paleolithic remains from the Iberian  
15  
16 Peninsula consist of isolated teeth or cranial remains (Pérez Iglesias, 2007, and references therein).  
17  
18  
19

20 We consider that the stratigraphic ascription of these teeth, rather than their morphology *per*  
21  
22 *se*, have contributed to incorrectly classify the published teeth from Axlor as belonging to  
23  
24 Neandertals. While Basabe (1973) considers that their general morphology resembles that of other  
25  
26 individuals found in Mousterian contexts, he still underlines their “evolved” status with the  
27  
28 presence of “intermediary characters” (Basabe, 1973:200), especially referring to the low degree of  
29  
30 taurodontism in the M<sup>1</sup> and the M<sup>2</sup>. The same author did classify the M<sup>1</sup> from Lezetxiki, which  
31  
32 shows the typical Neandertal occlusal morphology and a clear taurodontism (Basabe, 1970), as  
33  
34 belonging to a Neandertal individual.  
35  
36  
37

38 The second study that classified the Axlor teeth as Neandertals compared them with Sima de  
39  
40 los Huesos, Neandertals and modern humans both morphologically (using the data by Martín-  
41  
42 Torres et al., 2012) and metrically (using the data by Rodríguez-Cuenca (2003) and García-Bour,  
43  
44 Pérez-Pérez, & Chimenos (1997). However, most traits included in that study (Rostro-Carmona,  
45  
46 2013) are not taxonomically distinctive and, for those which are, the Axlor teeth show modern  
47  
48 human affinities. In terms of size, and using the data provided by Rostro-Carmona (2013), only the  
49  
50 canine would show a size closer to the Neandertal mean, the P<sup>4</sup> and M<sup>1</sup> would show intermediate  
51  
52 affinities while the size of the M<sup>2</sup> and M<sup>3</sup> would be more similar to modern humans. Our study  
53  
54 shows that, after including UPMHs in the comparative samples, and despite the overlap between  
55  
56 modern humans and Neandertals, the general size of the Axlor teeth is either non-determinant or  
57  
58  
59  
60



1  
2 more similar to modern humans. Finally, Rostro-Carmona (2013) used the presence of taurodontism  
3  
4 in the Axlor teeth to classify them as belonging to Neandertals, but our assessment indicates that the  
5  
6 Axlor teeth show a very limited degree of taurodontism, particularly when compared with classic  
7  
8 Neandertal molars.  
9

10  
11 The second group would encompass the cranial fragment and three additional tooth remains  
12  
13 that have clear Neandertal affinities and their stratigraphic position is secure within the Mousterian  
14  
15 levels. The bone thickness distribution pattern and endocranial anatomy of the cranial fragment are  
16  
17 consistent with Neandertal anatomy. Additionally, both incisors and the  $dm^2$  present characteristics  
18  
19 that allow us to ascribe them to Neandertals. Although heavily worn, the  $I_1$  shows Neandertal  
20  
21 affinities in its root configuration and proportions. Nevertheless, the CrPV and RpV values are  
22  
23 lower than the Neandertal values reported to date (Le Cabec et al., 2013; Becam & Chevalier,  
24  
25 2019). This might be related to an advanced age for the individual, as aging related deposition of  
26  
27 secondary dentine causes the reduction of the pulp channel (Aboshi, Takahashi, & Komuro, 2010;  
28  
29 Solheim, 1992). This would be consistent with the heavy wear present in this tooth. Second, both  
30  
31 the OES and EDJ of the deciduous upper incisor from Axlor present a set of characteristics  
32  
33 observed in other Neandertal specimens such as Portel-Ouest, La Ferrassie 8 (strong mesial and  
34  
35 distal marginal ridges, pronounced and asymmetric labial convexity) (Becam & Chevalier, 2019).  
36  
37 Third, although the  $dm^2$  does not show the typical Neanderthal skewed configuration, it does show  
38  
39 a notable development of the hypocone in relation to the metacone, the presence of the crista  
40  
41 obliqua, and a large Carabelli's tubercle at the OES and EDJ. These are common features to other  
42  
43 Neandertal  $dm^2$ s, such as Arrillor, La Ferrassie 8 or Portel-Ouest (Becam & Chevalier, 2019;  
44  
45 Bermúdez de Castro & Saenz de Buruaga, 1999). These new remains confirm the presence of  
46  
47 Neandertal fossil remains in Axlor, thus increasing the Neandertal hypodigm recovered in the  
48  
49 Eastern Cantabrian Region.  
50  
51  
52  
53  
54  
55  
56  
57  
58  
59  
60

1  
2 *Origin of the accumulation of the human fossil remains*  
3  
4  
5

6 Taphonomic and forensic analyses on hominin fossils are important to determine the origin of  
7 bone deposition and reconstruct the processes occurred during the fossil-diagenetic processes even  
8 for isolated fossils (Sanz et al., 2018). In some cases, it is even possible to determine causes of  
9 death (Sala et al., 2015) or drawing inferences about the mortuary practices of hominin groups, such  
10 as cannibalism (Rougier et al., 2016; Sala & Conard, 2016; Saladié et al., 2012; Saladié &  
11 Rodríguez-Hidalgo, 2017) or funerary activities (Gómez-Olivencia et al., 2018b).  
12  
13  
14  
15  
16  
17  
18  
19  
20  
21

22 In the case of the two deciduous teeth, they were lost by two different Neandertal individuals  
23 during the formation of levels V (left di<sup>1</sup>) and IV (right dm<sup>2</sup>). The presence of isolated deciduous  
24 teeth is not rare in Middle Paleolithic layers, and the closest example is found less than 25 km south  
25 from Axlor, in Arrillor (Figure 1; Bermúdez de Castro & Saénz de Buruaga, 1999; Iriarte-  
26 Chiapusso, Wood, & Sáenz de Buruaga, 2019), with other example from Le Portel Ouest (Becam &  
27 Chevalier, 2019). The cranial fragment from Axlor displays evidence of postmortem and  
28 perimortem fractures, but the absence of traces that could indicate the causes of such fractures  
29 makes it difficult to interpret its origin. Although we cannot rule out intentional causes for the  
30 perimortem fractures, the lack of clear anthropic cut marks or signs of anthropic manipulation does  
31 not allow us to go further in our interpretation. The absence of weathering could be interpreted as a  
32 non-aerial (or short-term) exposure of the fossils in the biostratigraphic phase. On the other hand,  
33 trampling has been documented on the cranial fragment suggesting certain displacement of the  
34 fossils which could be one of the explanations of the scarcity of human remains at the site.  
35  
36 Additionally, the Barandiarán collection shows some significant bias in comparison with the  
37 richness in fossil remains that we have observed at the site during recent excavations (Gómez-  
38 Olivencia et al., 2018a), in which smaller shaft fragments are absent. This bias could be a secondary  
39  
40  
41  
42  
43  
44  
45  
46  
47  
48  
49  
50  
51  
52  
53  
54  
55  
56  
57  
58  
59  
60

1  
2 reason of this scarcity. In this context, the recovery of additional human fossils in the Axlor site  
3  
4 would help elucidate the nature of these isolated remains found in a human occupation context.  
5  
6  
7

## 8 9 **Conclusions**

10  
11 Axlor (Dima, Biscay) is one of the most important Middle Paleolithic sites in the Cantabrian  
12  
13 region (northern Iberian Peninsula). The excavations performed by J.M. Barandiarán at the Axlor  
14  
15 site 50 years ago yielded a cranial vault fragment and eight teeth, five of which likely belonged to  
16  
17 the same individual, although two are currently lost. Three teeth (a left  $dm^2$ , a left  $di^1$ , and a right  $I_1$ )  
18  
19 and the cranial fragment show morphological features consistent with their classification as  
20  
21 Neandertals, and were found in undisturbed Mousterian context. However, the remaining three teeth  
22  
23 (plus two that have been lost since the initial finding), traditionally classified as Neandertals  
24  
25 (Basabe, 1973; Rostro Carmona, 2013), show morphological features and a general size more  
26  
27 compatible with their classification as modern humans. Moreover, the review of the original notes  
28  
29 by J.M. Barandiarán and our own observations during the recent excavations at the site suggest that  
30  
31 the archaeological context of these remains should be carefully reconsidered. We hypothesize that  
32  
33 these teeth may constitute one of the scarce examples of Upper Paleolithic remains in the Iberian  
34  
35 Peninsula, a hypothesis that would require a direct C14 dating to be tested, which currently is not  
36  
37 possible due to access limitations.  
38  
39  
40  
41  
42  
43  
44

## 45 **ACKNOWLEDGMENTS**

46  
47 We would like to thank I. García Camino (Arkeologi Museoa) for permission to study these  
48  
49 fossils. We thank L. García Boullosa for the cleaning of some of these fossils, and to the rest of the  
50  
51 Arkeologi Museoa staff. The Gobierno Vasco-Eusko Jaurlaritza granted the permission to micro-CT  
52  
53 these specimens. Thanks to the Jose Miguel de Barandiaran Fundazioa and Zuriñe Velez de  
54  
55 Mendizabal for the access to J.M. de Barandiarán's field notes. Thanks to B. Notario (CENIEH) for  
56  
57 help during the micro-CT scanning process. This research has also received support from the  
58  
59  
60

1  
2 Spanish Ministerio de Ciencia, Innovación y Universidades (proyecto PGC2018-093925-B-C33),  
3  
4 Research Group IT1418-19 from the Eusko Jaurlaritza-Gobierno Vasco. AGO was supported by  
5  
6 Ramón y Cajal fellowship (RYC-2017-22558). NS was supported by a Juan de la Cierva  
7  
8 Incorporación program (IJCI-2017-32804). Thanks also to our colleagues from BBP, UCM-ISCIH,  
9  
10 EHU-UPV, as well as to A. Rodríguez-Hidalgo and N. Weaver for stimulating discussions.  
11  
12  
13  
14

## 15 **Data Availability Statement**

16  
17  
18 The original micro-ct scans, the derived segmentation files, and 3D volumes are available in  
19  
20 figshare at <https://doi.org/10.6084/m9.figshare.10308272>.  
21  
22  
23

## 24 **ORCID**

25  
26  
27 *Asier Gómez-Olivencia* <https://orcid.org/0000-0001-7831-3902>

28  
29  
30 *Diego López-Onaindia* <https://orcid.org/0000-0002-5266-6416>

31  
32  
33 *Nohemi Sala* <https://orcid.org/0000-0002-0896-1493>

34  
35  
36 *Antoine Balzeau* <https://orcid.org/0000-0002-4226-611X>

37  
38  
39 *Ana Pantoja-Pérez* <https://orcid.org/0000-0001-9302-1756>

40  
41  
42 *Ignacio Arganda-Carreras* <https://orcid.org/0000-0003-0229-5722>

43  
44  
45 *Mikel Arlegi* <http://orcid.org/0000-0001-5665-9275>

46  
47  
48 *Joseba Rios-Garaizar* <https://orcid.org/0000-0001-8474-2156>

49  
50  
51 *Aida Gómez-Robles* <https://orcid.org/0000-0002-8719-2660>

## 52 **REFERENCES**

53  
54  
55  
56  
57 Aboshi, H., Takahashi, T., & Komuro, T. (2010). Age estimation using microfocus X-ray computed  
58  
59 tomography of lower premolars. *Forensic Science International*, 200, 35-40.  
60

- 1  
2 Albusu Andrade, C., Etxeberria Gabilondo, F., & Herrasti Erlogorri, L. (2014). Estudio de los restos  
3  
4 dentales humanos procedentes de la cueva de Santa Catalina. In E. Berganza Gochi, & J. L.  
5  
6 Arribas Pastor (Eds.). *La Cueva de Santa Catalina (Lekeitio): La intervención arqueológica*  
7  
8 *Restos vegetales, animales y humanos*, (pp. 361-365). Bilbao: Bizkaiko Foru Aldundia.
- 9  
10  
11 Altuna, J. (1989). La subsistance d'origine animal pendant le Moustérien dans la région Cantabrique  
12  
13 (Espagne). In M. Pathou, & L. G. Freeman (Eds.). *L'Homme de Neandertal La Subsistance*  
14  
15 *Actes du Colloque International de Liège*, vol 6, (pp. 41-43). Liège: ERAUL.
- 16  
17  
18 AlQahtani, S.J., Hector, M.P., & Liversidge, H.M. (2010). The London atlas of human tooth  
19  
20 development and eruption. *American Journal of Physical Anthropology*, 142, 481-490.
- 21  
22  
23 Arganda-Carreras, I., Kaynig, V., Rueden, C., Schindelin, J., Eliceiri, K. W., Cardona, A., &  
24  
25 Sebastian Seung, H. (2017). Trainable Weka Segmentation: a machine learning tool for  
26  
27 microscopy pixel classification. *Bioinformatics*, 33, 2424-2426.
- 28  
29  
30 Bayle, P., Le Luyer, M., & Robson Brown, K. A. (2017). The Palomas Dental Remains: Thickness  
31  
32 and Tissue Proportions. In E. Trinkaus, & M. J. Walker (Eds.). *Neandertals from the Sima*  
33  
34 *de las Palomas del Cabezo Gordo, Southeastern Spain*, (pp. 115-137). College Station,  
35  
36 Texas: Texas A&M University Press.
- 37  
38  
39 Bailey, S. E. (2002). A closer look at Neanderthal postcanine dental morphology: The mandibular  
40  
41 dentition. *The Anatomical Record*, 269, 148-156.
- 42  
43  
44 Bailey, S. E. (2004). A morphometric analysis of maxillary molar crowns of Middle-Late  
45  
46 Pleistocene hominins. *Journal of Human Evolution*, 47, 183-198.
- 47  
48  
49 Bailey, S. E., Benazzi, S., Souday, C., Astorino, C., Paul, K., & Hublin, J.-J. (2014). Taxonomic  
50  
51 differences in deciduous upper second molar crown outlines of *Homo sapiens*, *Homo*  
52  
53 *neanderthalensis* and *Homo erectus*. *Journal of Human Evolution*, 72, 1-9.
- 54  
55  
56 Balzeau, A. (2013). Thickened cranial vault and parasagittal keeling: Correlated traits and  
57  
58 autapomorphies of *Homo erectus*? *Journal of Human Evolution*, 64, 631-644.
- 59  
60

- 1  
2 Balzeau, A., Buck, L. T., Albessard, L., Becam, G., Grimaud-Hervé, D., Rae, T. C., & Stringer, C.  
3  
4 B. (2017). The Internal Cranial Anatomy of the Middle Pleistocene Broken Hill 1 Cranium.  
5  
6 *PaleoAnthropology*, 2017, 107-138.  
7  
8  
9 Balzeau, A., Grimaud-Hervé, D., & Gilissen, E. (2011). Where are inion and endinion? Variations  
10  
11 of the exo- and endocranial morphology of the occipital bone during hominin evolution.  
12  
13 *Journal of Human Evolution*, 61, 488-502.  
14  
15  
16 Barandiarán, I., & Cava, A. (2008). Identificaciones del Gravetiense en las estribaciones  
17  
18 occidentales del Pirineo: modelos de ocupación y uso. *Trabajos de Prehistoria*, 65, 13-28.  
19  
20  
21 Barandiarán, J. M. (1980). Excavaciones en Axlor. 1967-1974. In J. M. Barandiarán (Ed.). *Obras*  
22  
23 *Completas de José Miguel de Barandiarán Tomo XVII*, (pp. 127-384). Bilbao: La Gran  
24  
25 *Enciclopedia Vasca*.  
26  
27  
28 Basabe, J. M. (1970). Dientes humanos del paleolítico de Lezetxiki (Mondragón). *Munibe*, XXII,  
29  
30 113-124.  
31  
32  
33 Basabe, J. M. (1973). Dientes humanos del Musteriense de Axlor (Dima. Vizcaya). *Trabajos de*  
34  
35 *Antropología*, 16, 187-207.  
36  
37  
38 Basabe, J. M. (1982). Restos fósiles humanos de la región Vasco-Cantábrica. *Cuadernos de Sección*  
39  
40 *Antropología-Etnografía*, 1, 67-84.  
41  
42  
43 Becam, G., Chevalier, T., Gregoire, S., Braga, J., Balzeau, A., De Lumley, M.A., Vezian, R. 2015.  
44  
45 The characterization of the outer enamel surface and the enamel dentine junction of  
46  
47 deciduous and permanent Neandertal teeth from Le Portel-Ouest cave (Ariège, France).  
48  
49 *1840<sup>ème</sup> Journée de la Société d'Anthropologie de Paris*.  
50  
51  
52 Becam, G., & Chevalier, T. (2019). Neandertal features of the deciduous and permanent teeth from  
53  
54 Portel-Ouest Cave (Ariège, France). *American Journal of Physical Anthropology*, 168, 45-  
55  
56 69.  
57  
58  
59 Becam, G., Verna, C., Gómez-Robles, A., Gómez-Olivencia, A., Albessard, L., Arnaud, J., . . .  
60  
Balzeau, A. (2019). Isolated teeth from La Ferrassie: Reassessment of the old collections,

1  
2 new remains, and their implications. *American Journal of Physical Anthropology*, 169, 132-  
3  
4 142.

5  
6 Behrensmeyer, A. K. (1978). Taphonomic and ecologic information from bone weathering.  
7  
8 *Paleobiology*, 4, 150-162.

9  
10 Bermúdez de Castro, J. M., & Sáenz de Buruaga, A. (1999). Étude Préliminaire du site Pléistocène  
11  
12 Supérieur à hominidé d'Arrillor (Pays Basque, Espagne). *L'Anthropologie*, 103, 633-639.

13  
14 Carlsen, O. (1987). Dental Morphology. Copenhagen: Munksgaard.

15  
16 Carretero, J. M., Quam, R. M., Gómez-Olivencia, A., Castilla, M., Rodríguez, L., & García-  
17  
18 González, R. (2015). The Magdalenian human remains from El Mirón Cave, Cantabria  
19  
20 (Spain). *Journal of Archaeological Science*, 60, 10-27.

21  
22 Castaños, P. M. (2005). Revisión actualizada de las faunas de macromamíferos del Würm antiguo  
23  
24 en la Región Cantábrica. In J. A. Lasheras, & R. Montes (Eds.). Neandertales cantábricos,  
25  
26 estado de la cuestión, (pp. 201-207). Santander: Museo de Altamira.

27  
28 de la Rúa, C., & Hervella, M. (2011). Estudio antropológico de los dientes humanos de la cueva de  
29  
30 Aitzbitarte III (Rentería. Gipuzkoa) (Paleolítico superior). In J. Altuna, K. Mariezkurrena, &  
31  
32 J. Rios (Eds.). Ocupaciones humanas en Aitzbitarte III (País Vasco) 33600-18400 BP (Zona  
33  
34 de entrada a la cueva), (pp. 385-393). Vitoria-Gasteiz: Eusko Jaurlaritza-Gobierno Vasco.

35  
36 Domínguez-Rodrigo, M., de Juana, S., Galán, A. B., & Rodríguez, M. (2009). A new protocol to  
37  
38 differentiate trampling marks from butchery cut marks. *Journal of Archaeological Science*,  
39  
40 36, 2643-2654.

41  
42 Duarte, C., Maurício, J., Souto, P., Pettitt, P. B., Trinkaus, E., Van Plicht, H. D., & Zilhão, J.  
43  
44 (1999). The early Upper Paleolithic human skeleton from the Abrigo do Lagar Velho  
45  
46 (Portugal) and modern human emergence in Iberia. *Proceedings of the National Academy of  
47  
48 Sciences of the United States of America*, 96, 7604-7609.

- 1  
2 Fu, Q., Hajdinjak, M., Moldovan, O. T., Constantin, S., Mallick, S., Skoglund, P., . . . Pääbo, S.  
3  
4 (2015). An early modern human from Romania with a recent Neanderthal ancestor. *Nature*,  
5  
6 524, 216-219.  
7  
8  
9 García-Bour, J., Pérez-Pérez, A., & Chimenos, E. (1997). Evolución de la dentición en la transición  
10  
11 mesolítico-neolítico de la península ibérica; un modelo de sustitución poblacional. *Anales*  
12  
13 *de Odontoestomatología*, 3, 116-121.  
14  
15  
16 Garralda, M. D. (2005). Los Neandertales en la Península Ibérica. *Munibe (Antropología*  
17  
18 *Arkeologia)*, 57, 289-314.  
19  
20  
21 Garralda, M.-D., Maíllo-Fernández, J.-M., Higham, T., Neira, A., & Bernaldo de Quirós, F. (in  
22  
23 press). The Gravettian child mandible from El Castillo Cave (Puente Viesgo, Cantabria,  
24  
25 Spain). *American Journal of Physical Anthropology*. <https://doi.org/10.1002/ajpa.23906>  
26  
27  
28 Gómez-Olivencia, A., Quam, R., Sala, N., Bardey, M., Ohman, J. C., & Balzeau, A. (2018b). La  
29  
30 Ferrassie 1: New perspectives on a “classic” Neandertal. *Journal of Human Evolution*, 117,  
31  
32 13-32.  
33  
34  
35 Gómez-Olivencia, A., Sala, N., Núñez-Lahuerta, C., Sanchis, A., Arlegi, M., & Rios-Garaizar, J.  
36  
37 (2018a). First data of Neandertal bird and carnivore exploitation in the Cantabrian Region  
38  
39 (Axlor; Barandiaran excavations; Dima, Biscay, Northern Iberian Peninsula). *Scientific*  
40  
41 *Reports*, 8, 10551.  
42  
43  
44 Gómez-Robles, A., Bermúdez de Castro, J. M., Martínón-Torres, M., Prado-Simón, L., & Arsuaga,  
45  
46 J. L. (2012). A geometric morphometric analysis of hominin upper second and third molars,  
47  
48 with particular emphasis on European Pleistocene populations. *Journal of Human*  
49  
50 *Evolution*, 63, 512-526.  
51  
52  
53 Gómez-Robles, A., Martínón-Torres, M., Bermúdez de Castro, J. M., Margvelashvili, A., Bastir,  
54  
55 M., Arsuaga, J. L., . . . Martínez, L. M. (2007). A geometric morphometric analysis of  
56  
57 hominin upper first molar shape. *Journal of Human Evolution*, 53, 272-285.  
58  
59  
60



- 1  
2 Gómez-Robles, A., Martín-Torres, M., Bermúdez de Castro, J. M., Prado-Simón, L., & Arsuaga,  
3  
4 J. L. (2011). A geometric morphometric analysis of hominin upper premolars. Shape  
5  
6 variation and morphological integration. *Journal of Human Evolution*, 61, 688-702.  
7  
8  
9 González Echegaray, J., & Freeman, L. G. (1973). Cueva Morín: Excavaciones 1969. Santander:  
10  
11 Publicaciones del Patronato de las Cuevas Prehistóricas de la Provincia de Santander.  
12  
13 González Echegaray, J., García Guinea, M. A., Begines Ramírez, A., & Madariaga de la Campa, B.  
14  
15 (1963). Cueva de la Chora (Santander). Madrid: Ministerio de Educación Nacional.  
16  
17 Dirección General de Bellas Artes. Servicio Nacional de Excavaciones Arqueológicas.  
18  
19  
20 González Echegaray, J., & Ripoll Perelló, E. (1954). Hallazgos en la cueva de La Pasiega (Puente  
21  
22 Viesgo, Santander). *Ampurias*, XV-XVI, 43-65.  
23  
24  
25 González-Urquijo, J. E., Ibañez, J. J., Lazuén, T., & Mozota, M. (2014). Axlor. In R. Sala (Ed.).  
26  
27 Los Cazadores Recolectores Del Pleistoceno Y Del Holoceno En Iberia Y El Estrecho de  
28  
29 Gibraltar, (pp. 45-48). Burgos: Universidad de Burgos.  
30  
31  
32 Grimaud-Hervé, D. (1997). L'évolution de l'encéphale chez *Homo erectus* et *Homo sapiens*:  
33  
34 exemples de l'Asie et de l'Europe: CNRS ed. Paris.  
35  
36  
37 Guerrero Sala, L. A., & Lorenzo Lizalde, J. L. (1981). Antropología física en Rascaño. In J.  
38  
39 González Echegaray, & I. Barandiarán Maestu, (Eds.), *El Paleolítico Superior de la Cueva*  
40  
41 *de Rascaño (Santander)* (pp. 278-). Santander: Ministerio de Cultura. Dirección General de  
42  
43 Bellas Artes, Archivos y Bibliotecas.  
44  
45  
46 Henry-Gambier, D. (2006). Les sépultures de Sorde-l'Abbaye (Landes). In M. Dachary, (Ed.), *Les*  
47  
48 *Magdaléniens à Duruthy Qui étaient-ils, comment vivaient-ils?* (pp. 67-73). Mont-de-  
49  
50 Marsan: Conseil général des Landes.  
51  
52  
53 Henry-Gambier, D., Normand, C., & Pétilon, J.-M. (2013). Datation radiocarbone directe et  
54  
55 attribution culturelle des vestiges humains paléolithiques de la grotte d'Isturitz (Pyrénées-  
56  
57 Atlantiques). *Bulletin de la Société préhistorique française*, 110, 645-656.  
58  
59  
60

- 1  
2 Iriarte-Chiapusso, M. J., Wood, R., & Sáenz de Buruaga, A. (2019). Arrillor cave (Basque Country,  
3 northern Iberian Peninsula). Chronological, palaeo-environmental and cultural notes on a  
4 long Mousterian sequence. *Quaternary International*, *508*, 107-115.  
5  
6  
7  
8  
9 Jarvis, A., Reuter, H. I., Nelson, A., & Guevara, E. (2008). Hole-filled SRTM for the globe Version  
10 4. available from the CGIAR-CSI SRTM 90m Database (<http://srtm.csi.cgiar.org>), *15*, 25-  
11 54.  
12  
13  
14  
15  
16 Le Cabec, A., Gunz, P., Kupczik, K., Braga, J., & Hublin, J.-J. (2013). Anterior tooth root  
17 morphology and size in Neanderthals: Taxonomic and functional implications. *Journal of*  
18 *Human Evolution*, *64*, 169-193.  
19  
20  
21  
22  
23 Legland, D., Arganda-Carreras, I., & Andrey, P. (2016). MorphoLibJ: integrated library and plugins  
24 for mathematical morphology with ImageJ. *Bioinformatics*, *32*, 3532-3534.  
25  
26  
27  
28 Marín-Arroyo, A. B., Rios-Garaizar, J., Straus, L. G., Jones, J. R., de la Rasilla, M., González  
29 Morales, M. R., . . . Ocio, D. (2018). Chronological reassessment of the Middle to Upper  
30 Paleolithic transition and Early Upper Paleolithic cultures in Cantabrian Spain. *Plos one*, *13*,  
31 e0194708.  
32  
33  
34  
35  
36  
37 Martin, R. M. G., Hublin, J.-J., Gunz, P., & Skinner, M. M. (2017). The morphology of the enamel-  
38 dentine junction in Neanderthal molars: Gross morphology, non-metric traits, and temporal  
39 trends. *Journal of Human Evolution*, *103*, 20-44.  
40  
41  
42  
43  
44 Martinón-Torres, M., Bermúdez de Castro, J. M., Gómez-Robles, A., Prado-Simón, L., & Arsuaga,  
45 J. L. (2012). Morphological description and comparison of the dental remains from  
46 Atapuerca-Sima de los Huesos site (Spain). *Journal of Human Evolution*, *62*, 7-58.  
47  
48  
49  
50  
51 Molnar, S. (1971). Human tooth wear, tooth function and cultural variability. *American Journal of*  
52 *Physical Anthropology*, *34*, 175-190.  
53  
54  
55  
56  
57  
58  
59  
60 Obermaier, H. (1925). El hombre fósil. Madrid: Ediciones Istmo.

- 1  
2 Pan, L., & Zanolli, C. (2019). Comparative observations on the premolar root and pulp canal  
3 configurations of Middle Pleistocene Homo in China. *American Journal of Physical*  
4 *Anthropology*, 168, 637-646.  
5  
6  
7  
8 Pérez-Iglesias, J. M. (2007). Restos fósiles humanos en el Paleolítico superior de la península  
9 ibérica. *Arqueoweb*, 8, 1-17.  
10  
11  
12 QGIS Development Team, 2009. QGIS Geographic Information System. Open Source Geospatial  
13 Foundation. URL <http://qgis.org>  
14  
15  
16 Rios-Garaizar, J. (2017). A new chronological and technological synthesis for Late Middle  
17 Paleolithic of the Eastern Cantabrian Region. *Quaternary International*, 433, 50-63.  
18  
19  
20 Rodríguez Cuenca, J. V. (2003). Dientes y diversidad humana: avances de la antropología dental.  
21 Bogotá: Editora Guadalupe Ltda.  
22  
23  
24 Rostro Carmona, J. (2013). Estudio comparado de las piezas dentales de *Homo neanderthalensis* del  
25 yacimiento Musteriense de Axlor (Dima, Vizcaya). *CKQ Estudios de*  
26 *Cuaternario/Kuaternario Ikasketak/Quaternary Studies*, 3, 91-100.  
27  
28  
29 Rougier, H., Crevecoeur, I., Beauval, C., Posth, C., Flas, D., Wißing, C., . . . Krause, J. (2016).  
30 Neandertal cannibalism and Neandertal bones used as tools in Northern Europe. *Scientific*  
31 *Reports*, 6, 29005.  
32  
33  
34 Sala, N., & Conard, N. (2016). Taphonomic analysis of the hominin remains from Swabian Jura and  
35 their implications for the mortuary practices during the Upper Paleolithic. *Quaternary*  
36 *Science Reviews*, 150, 278-300.  
37  
38  
39 Sala, N., Pantoja-Pérez, A., Arsuaga, J. L., Pablos, A., & Martínez, I. (2016). The Sima de los  
40 Huesos Crania: Analysis of the cranial breakage patterns. *Journal of Archaeological*  
41 *Science*, 72, 25-43.  
42  
43  
44 Saladié, P., Huguet, R., Rodríguez-Hidalgo, A., Cáceres, I., Esteban-Nadal, M., Arsuaga, J. L., . . .  
45 Carbonell, E. (2012). Intergroup cannibalism in the European Early Pleistocene: The range  
46 expansion and imbalance of power hypotheses. *Journal of Human Evolution*, 63, 682-695.  
47  
48  
49  
50  
51  
52  
53  
54  
55  
56  
57  
58  
59  
60

- 1  
2 Saladié, P., & Rodríguez-Hidalgo, A. (2017). Archaeological Evidence for Cannibalism in  
3  
4 Prehistoric Western Europe: from Homo antecessor to the Bronze Age. *Journal of*  
5  
6 *Archaeological Method and Theory*, 24, 1034-1071.  
7  
8  
9 Sanguino González, J., & Montes Barquín, r. (2005). Nuevos datos para el conocimiento del  
10  
11 Paleolítico Medio en el centro de la Región Cantábrica: la cueva de Covalejos (Piélagos,  
12  
13 Cantabria). In R. Montes Barquín, & J. A. Lasheras Corruchaga, (Eds.), *Actas de la Reunión*  
14  
15 *científica: Neandertales cantábricos, estado de la cuestión* (pp. 489-538). Santander: Museo  
16  
17 Nacional y Centro de Investigación de Altamira. Ministerio de Cultura.  
18  
19  
20 Sanz M., Sala N., Daura J., Pantoja-Pérez A., Santos E, Zilhão J, and Arsuaga JL. (2018).  
21  
22 Taphonomic inferences about Middle Pleistocene hominins: The human cranium of Gruta  
23  
24 da Aroeira (Portugal). *American Journal of Physical Anthropology*, 167, 615-627.  
25  
26  
27 Schindelin, J., Arganda-Carreras, I., Frise, E., Kaynig, V., Longair, M., Pietzsch, T., . . . Cardona,  
28  
29 A. (2012). Fiji: an open-source platform for biological-image analysis. *Nature Methods*,  
30  
31 9,676.  
32  
33  
34 Solheim, T. (1992). Amount of secondary dentin as an indicator of age. *European Journal of Oral*  
35  
36 *Sciences*, 100, 193-199.  
37  
38  
39 Tejero, J. M., Avezuela, B., White, R., Ranlett, S., Quam, R., Tattersall, I., & Bernaldo de Quirós,  
40  
41 F. (2010). Un pedazo de la Prehistoria cántabra en Nueva York. Las Colecciones de la  
42  
43 Cueva de El Castillo (Puente Viesgo, Cantabria) en el American Museum of Natural History  
44  
45 (Nueva York, EEUU). *Munibe (Antropología-Arkeología)*, 61, 5-16.  
46  
47  
48 Turner, C. G., Nichol, C. R., & Scott, G. R. (1991). Scoring procedures for key morphological traits  
49  
50 of the permanent dentition: the Arizona State University dental anthropology system. In M.  
51  
52 Kelley, & C. Larsen (Eds.). *Advances in Dental Anthropology*, (pp. 13-31). New York:  
53  
54 Wiley-Liss.  
55  
56  
57 Vallois, H., & Delmas, L. (1976). Los frontales de la cueva de El Castillo (España). *Trabajos de*  
58  
59 *Prehistoria*, 33, 113-120.  
60

1  
2 Zapata, J., Bayle, P., Lombardi, A. V., Pérez-Pérez, A., & Trinkaus, E. (2017). The Palomas Dental  
3  
4 Remains: Preservation, Wear, and Morphology. In E. Trinkaus, & M. J. Walker (Eds.),  
5  
6 *Neandertals from the Sima de las Palomas del Cabezo Gordo, Southeastern Spain* (pp. 52-  
7  
8 88). College Station, Texas: Texas A&M University Press.  
9  
10  
11  
12  
13  
14  
15  
16  
17  
18  
19  
20  
21  
22  
23  
24  
25  
26  
27  
28  
29  
30  
31  
32  
33  
34  
35  
36  
37  
38  
39  
40  
41  
42  
43  
44  
45  
46  
47  
48  
49  
50  
51  
52  
53  
54  
55  
56  
57  
58  
59  
60

## Figure legends

**FIGURE 1** Location of Axlor (red star) and other Paleolithic sites with human remains in the Center and East of the Cantabrian Region (northern Iberian Peninsula and southwestern France). 1: La Pasiega (González Echegaray & Ripoll Perelló, 1954); 2: Castillo (N; HS; Garralda, 2005; Garralda, Maíllo-Fernández, Higham, Neira, & Bernaldo de Quirós, in press; Obermaier, 1925; Tejero et al., 2010; Vallois & Delmas, 1976; 3 Covalejos (N, HS; Sanguino González & Montes Barquín, 2005); 4: Pendo (Basabe, 1982); 5: Morín (HS; González Echegaray & Freeman, 1973; Obermaier, 1925); 6: Rascaño (Guerrero Sala & Lorenzo Lizalde, 1981); 7: La Chora (González Echegaray, García Guinea, Begines Ramírez & Madariaga de la Campa, 1963); 8: Mirón (HS; Carretero et al., 2015); 9: Arrillor (N, Bermúdez de Castro & Sáenz de Buruaga, 1999); 10: Axlor (N; HS; this work); 11: Lezetxiki (N; Basabe, 1970); 12: Santa Catalina (HS; Albisu Andrade, Etxeberria Gabilondo, & Herrasti Erlogorri, 2014); 13: Aitzbitarte III (HS; de la Rúa & Hervella, 2011); 14: Alkerdi (Barandiarán & Cava, 2008); 15: Isturitz (HS; Henry-Gambier, Normand, & Pétilion, 2013); 16: Duruthy (HS; Henry-Gambier, 2006). N=Neandertal; HS=*Homo sapiens*. Base map made with QGIS 2.18.17 (QGIS Development Team, 2009) with data by Jarvis, Reuter, Nelson, & Guevara (2008).

**FIGURE 2** Excavation plan (a) and stratigraphic column (b) of Axlor cave (modified from Gómez-Olivencia et al., 2018a). (a) In the excavation plan the grid system used by J.M. Barandiarán (black square and white numbers) and the excavation area is shadowed in gray. The grid system used by the recent excavations is marked using black letters and numbers and the excavation area is outlined using a thick black line. The dotted line represents the rock-shelter wall when the site was first excavated, during the excavation this wall went back, revealing a possible cave infilling. The colors correspond to the levels to which these remains were attributed based on the notes by

1  
2 Barandiarán. (b) Synthetic section of the 1967–1974 excavation stratigraphy, drawn from the  
3  
4 description of the layers by J. M. Barandiarán (1980). Different levels are marked with different  
5  
6 colors, and the human remains are marked by silhouettes.  
7  
8  
9

10  
11 **FIGURE 3** Ax.11B.415.400 left parietal fragment. The original fossil and the 3D model are  
12  
13 shown on different views. On the lower row, the approximate location of this fragment is shown on  
14  
15 the La Ferrassie 1 Neandertal cranium (left), a thickness map (from 2 to 12 mm) is shown (middle)  
16  
17 with PC that correspond to thicker bone where is located the postcentral sulcus and V to a relative  
18  
19 thinning produced by the anterior ramus of the meningeal system; and the anatomical features on  
20  
21 the endocranial surface (right): including meningeal veins, A = anterior branch, O = obelic branch,  
22  
23 and sulcal imprints C = central sulcus, PC = postcentral sulcus.  
24  
25  
26  
27  
28

29  
30 **FIGURE 4** Ectocranial view of the specimen Ax.11B.415.400 with the location of zones a-d,  
31  
32 and detailed images of these zones, where striations are located. In some cases, the grooves show a  
33  
34 close “V” shape but do not show microstriations. The general morphology of these grooves (see  
35  
36 text) make them compatible with trampling marks.  
37  
38  
39  
40

41  
42 **FIGURE 5** Dental remains previously studied by Basabe (1973) and Rostro-Carmona (2013),  
43  
44 and likely belonging to the same individual. The teeth are shown in mesial, buccal, distal, lingual  
45  
46 (top) and occlusal (bottom) views, together with the results of the enamel segmentation and the EDJ  
47  
48 surface morphology. Pulp chamber volumes (in blue) are shown in mesial ( $P^4$ ,  $M^1$ ) and lingual ( $M^2$ )  
49  
50 views. A virtual reconstruction of the teeth in buccal and occlusal views is also provided. Scale bars  
51  
52 = 1 cm.  
53  
54  
55  
56

57  
58 **FIGURE 6** Principal components analysis of shape (left column) and form variation (right  
59  
60 column), corresponding to the teeth previously studied by Basabe (1973) and Rostro-Carmona

1  
2 (2013), and likely belonging to the same individual. The Axlor remains have been compared to  
3  
4 Neandertals (NEA), fossil *Homo sapiens* (FSAP) and recent *Homo sapiens* (RSAP). In both form  
5  
6 and shape space, the Axlor remains align more closely with modern humans. TPS-grids show  
7  
8 anatomical variation corresponding to the positive and negative extreme of each PC when all the  
9  
10 other PCs are held equal to 0. For M<sup>1</sup> variation, the two data points correspond to Axlor's variation  
11  
12 before (darker red) and after (lighter red) correcting the enamel cracks ([Supplementary information](#)  
13  
14 [Figure S13](#)).  
15  
16  
17  
18  
19

20 **FIGURE 7** New dental remains from the Barandiarán collection of Axlor. AX.5B.299.16 (right  
21  
22 permanent first lower incisor, I<sub>1</sub>): root canal morphology (blue) in mesial view; mesial, buccal,  
23  
24 distal, lingual and occlusal views. AX.5B.299.31.64.17 (upper left first deciduous incisor, dI<sup>1</sup>): top,  
25  
26 mesial, buccal, distal, lingual and occlusal views. AX.9E.283.103 (left dM<sup>2</sup>): top, mesial, buccal,  
27  
28 distal, lingual and occlusal views. In the virtual reconstructions, enamel is represented in white and  
29  
30 dentine in brown. Scale bars = 1 cm  
31  
32  
33  
34  
35  
36  
37  
38  
39  
40  
41  
42  
43  
44  
45  
46  
47  
48  
49  
50  
51  
52  
53  
54  
55  
56  
57  
58  
59  
60



Table 1

Inventory of the Axlor human remains found during the Barandiarán excavations.

Label	Year	Archaeological context <sup>a</sup>	Revised archaeological context	Museum data base (MDB)/Basabe, 1973 (B)	Present study	Figure
Ax.13F.265.1 <sup>a</sup> Ax.13E/13F.265-270.3 <sup>b</sup>	1967	Level IV (Mousterian)	Doubtful	Neandertal (MDB) Left P <sup>4</sup> (B)	Modern human Left P <sup>4</sup>	Figure 5
Ax.13F.265.3 <sup>a</sup> Ax.13E/13F.265-270.3 <sup>b</sup>	1967	Level IV (Mousterian)	Doubtful	Neandertal (MDB) Left maxillary fragment with M <sup>1</sup> (B)	Modern human Left maxillary fragment with M <sup>1</sup>	Figure 5
Ax.13F.265.3 <sup>a</sup>	1967	Level IV (Mousterian)	Doubtful	Left M <sup>2</sup> (B)	Specimen lost	-
Ax.13F.265.2 <sup>a</sup> Ax.13E/13F.265-270.3	1967	Level IV (Mousterian)	Doubtful	Neandertal (MDB) Left M <sup>3</sup> (B)	Modern human Left M <sup>3</sup>	Figure 5
Ax.13E.285.3 <sup>a</sup>	1967	Level IV (Mousterian)	Doubtful	Left C' (B)	Specimen lost	-
Ax.11B.415.9 <sup>a</sup> Ax.11B.415.400 (physical label: Ax.11B.415)b	1969	Level VIII (Mousterian)	Mousterian	Human cranial fragment (MDB) Neandertal (MDB)	Neandertal Left parietal bone	Figure 3
Ax.9E.283.103	1973 or 1974	Level IV (Mousterian)	Mousterian	Fauna (indeterminate taxon) (MDB)	Neandertal Right dm <sup>2</sup>	Figure 7
Ax.5B.299.31.64.17	1974	Level V (Mousterian)	Mousterian	Human tooth (MDB)	Neandertal Left di <sup>1</sup>	Figure 7
Ax.5B.299.16	1974	Level V (Mousterian)	Mousterian	Human tooth (MDB)	Neandertal Adult right I <sub>1</sub>	Figure 7

<sup>a</sup> Based on the information provided by J.M. de Barandiarán field notes. The M<sup>1</sup> and the M<sup>2</sup> were found together.

<sup>b</sup> Based on the information provided by the Arkeologi Museoa (Bilbao, Biscay).

1  
2 \*\* Virtual (not written) label  
3  
4  
5  
6  
7  
8  
9  
10  
11  
12  
13  
14  
15  
16  
17  
18  
19  
20  
21  
22  
23  
24  
25  
26  
27  
28  
29  
30  
31  
32  
33  
34  
35  
36  
37  
38  
39  
40  
41  
42  
43  
44  
45  
46  
47  
48  
49  
50  
51  
52  
53  
54  
55  
56  
57  
58  
59  
60

Table 2

Comparison of external crown metric data between Axlor teeth and Neandertals, Upper Paleolithic modern humans (UPMH), and recent modern humans (RMH).

Tooth	Variable	Axlor			Neandertals <sup>a</sup>					Upper Palaeolithic modern humans <sup>a</sup>					Recent modern humans <sup>a</sup>				
		This study	Rostro-Carmona, 2013	Basabe, 1973	Mean	SD	Min	Max	<i>n</i>	Mean	SD	Min	Max	<i>n</i>	Mean	SD	Min	Max	<i>n</i>
C	M-D	-	-	8.0	8.74	0.67	7.40	10.00	31	8.06	0.58	6.90	9.50	36	7.58	0.43	6.80	8.5	38
	B-L	-	-	9.2	9.92	0.65	8.40	11.40	34	9.02	0.77	7.50	10.74	38	8.26	0.68	7.20	9.4	38
P <sup>4</sup>	M-D	6.6	6.7	6.6	7.49	0.78	6.10	8.80	30	6.84	0.52	5.90	7.90	38	6.45	0.46	5.50	7.5	38
	B-L	9.7	9.8	9.7	10.39	0.70	9.00	11.70	34	9.69	0.69	7.50	11.29	38	9.04	0.49	8.10	9.9	38
M <sup>1</sup>	M-D	9.8	10.2	10.0	11.61	1.09	9.30	13.60	28	10.71	0.71	8.40	12.30	41	10.03	0.52	8.40	11.4	42
	B-L	11.1	11.2	11.8	12.34	0.70	11.10	14.20	33	12.12	0.63	10.00	13.98	42	11.27	0.56	10.20	12.5	42
M <sup>2</sup>	M-D	-	-	9.3	10.84	1.23	9.10	15.90	34	10.10	0.72	8.90	11.80	41	9.22	0.66	7.80	10.5	41
	B-L	-	-	10.0	12.60	0.94	10.54	14.60	38	12.27	0.90	8.30	14.00	42	11.35	0.84	9.90	13.9	41
M <sup>3</sup>	M-D	8.7	8.6	8.6	9.74	0.94	6.80	11.35	30	9.01	1.09	7.00	11.60	39	8.55	0.84	7.30	10.5	30
	B-L	10.2	10.1	10.0	11.96	1.16	7.70	14.25	30	11.40	1.10	6.90	13.30	40	10.88	0.98	9.30	13.2	30
I <sub>1</sub>	M-D	4.8	-	-	5.73	0.44	4.92	6.35	24	5.51	0.60	3.70	6.60	22	5.24	0.45	4.60	6.7	31
	B-L	7.7	-	-	7.37	0.51	6.10	8.15	29	6.23	0.45	5.30	7.10	42	6.03	0.44	5.10	6.8	32
di <sup>1</sup>	M-D	7.6	-	-	7.03	0.81	5.60	8.00	11	6.85	0.77	6.20	7.70	4					
	B-L	6.0	-	-	5.67	0.48	4.70	6.20	11	5.30	0.29	4.90	5.70	5					
dm <sup>2</sup>	M-D	(9.0)	-	-	9.18	0.70	8.00	10.40	15	9.19	0.30	8.97	9.40	2					
	B-L	10.3	-	-	10.14	0.57	9.00	11.10	16	10.32	0.57	9.90	11.10	4					

B-L= Bucco-lingual; M-D = Mesio-distal. Values between parentheses are estimated.

The C\*, P<sup>4</sup>, M<sup>1</sup>, M<sup>2</sup> and M<sup>3</sup> were firstly published by Basabe (2013) and are from the same individual.

<sup>a</sup>For sample information see [Supplementary Information Table S5](#).

Table 3

Comparison of non-metric traits at the occlusal enamel surface (OES), at the enamel-dentine junction (EDJ) and root number between the P<sup>4</sup> and Neandertals, Upper Paleolithic modern humans (UPMH), and recent modern humans (RMH).

Tooth region	Trait	Grade for Axlor	Neandertals		UPMH		RMH	
			<i>n</i>	%	<i>n</i>	%	<i>n</i>	%
OES	Transverse crest	Absent	2/16	12.4	2/11	18.2	0/113	0.0
	Buccal essential crest (BEF)	2	10/15	66.6	4/11*	36.4	10/106	9.4
	Lingual essential crest (LEF)	NO	11/14	78.6	0/11	0.0	9/108	8.3
	BMaxPAR	1 (Dist)	5/12	41.7	5/9	55.6	18/88	20.5
EDJ	Transverse crest	2 (continuous, but not complete)	9/13	69.2	0/1	0.0	2/14	14.3
	Buccal essential crest	2 (bifurcated)	8/13	61.5	0/1	0.0	4/20	20.0
	Lingual essential crest	2 (bifurcated)	12/13	92.3	0/1	0.0	0/20	0.0
	Distal accessory ridge	1 (present)	5/13	38.4	0/1	0.0	12/20	60.0
	Mesial accessory ridge	0 (absent)	8/13	61.5	1/1	100.0	8/20	40.0
	Mesial accessory cusp	0 (absent)	13/13	100.0	1/1	100.0	20/20	100.0
	Distal accessory cusp	0 (absent)	10/13	76.9	1/1	100.0	20/20	100.0
Root	Root canal type	1R <sub>1</sub>	1/10	10.0	-	-	4/13	30.8

OES trait frequencies from Martín-Torres et al. (2012); EDJ data from Becam et al. (2019); Root channel data from Bayle, Le Luyer, & Robson Brown (2017; Las Palomas 53 and 68 left P<sup>4</sup>s), Zapata, Bayle, Lombardi, Pérez-Pérez, & Trinkaus (2017), and Pan & Zanolli (2019).

1  
2  
3  
4  
5  
6  
7  
8  
9  
10  
11  
12  
13  
14  
15  
16  
17  
18  
19  
20  
21  
22  
23  
24  
25  
26  
27  
28  
29  
30  
31  
32  
33  
34  
35  
36  
37  
38  
39  
40  
41  
42  
43  
44  
45  
46  
47  
48  
49  
50  
51  
52  
53  
54  
55  
56  
57  
58  
59  
60

Table 4

Comparison of non-metric traits at the occlusal enamel surface (OES) and enamel-dentine junction (EDJ) between the Axlor M<sup>1</sup>, Neandertals, Upper Paleolithic modern humans (UPMH) and recent modern humans (RMH).

Tooth region	Trait	Grade for Axlor	Neandertals		UPMH		RMH	
			<i>n</i>	%	<i>n</i>	%	<i>n</i>	%
OES	Metacone	4	13/23	56.5	11/19	57.9	73/127	57.5
	Hypocone	4	10/23	43.5	10/19	52.6	58/127	45.7
	Cusp 5	0	1/22	4.5	1/18	5.6	44/125	35.2
	Parastyle	0	14/20	70.0	15/15	100.0	121/123	98.4
EDJ	Crista Obliqua	Type II	2/19	10.0	-	-	1/12	8.3
	Post Paracone	Intermediate	10/19	52.6	-	-	0/12	0.0

OES trait frequencies from Martín-Torres et al. (2012); EDJ data from Martin et al. (2017; combining data from early and late Neandertals together).

Table 5

Comparison of non-metric traits at the occlusal enamel surface (OES) and enamel-dentine junction (EDJ) between the Axlor M<sup>3</sup>, Neandertals, Upper Paleolithic modern humans (UPMH) and recent modern humans (RMH).

Tooth region	Trait	Grade for Axlor	Neandertals		UPMH		RMH	
			<i>n</i>	%	<i>n</i>	%	<i>n</i>	%
OES	Metacone	>3	9/18	50.0	5/10	50.0	58/93	62.4
	Hypocone	0	3/17	17.6	2/10	20.0	15/93	16.1
	Cusp 5	1	1/17	5.9	1/10	10.0	4/93	4.3
	Carabelli	0	12/15	80.0	5/9	55.6	68/89	76.4
	Parastyle	0	14/16	87.5	9/9	100	81/88	92.0
EDJ	Crista Obliqua	absent	0/12	0.0	-	-	3/7	42.9
	Post Paracone	intermediate	1/12	8.3	-	-	2/7	28.6

OES trait frequencies from Martín-Torres et al. (2012); EDJ data from Martín et al. (2017; combining data from early and late Neandertals together).



FIGURE 1 Location of Axlor (red star) and other Paleolithic sites with human remains in the Center and East of the Cantabrian Region (northern Iberian Peninsula and southwestern France). 1: La Pasiega (González Echegaray & Ripoll Perelló, 1954); 2: Castillo (N; HS; Garralda, 2005; Garralda, Maíllo-Fernández, Higham, Neira, & Bernaldo de Quirós, in press; Obermaier, 1925; Tejero et al., 2010; Vallois & Delmas, 1976); 3: Covalejos (N, HS; Sanguino González & Montes Barquín, 2005); 4: Pendo (Basabe, 1982); 5: Morín (HS; González Echegaray & Freeman, 1973; Obermaier, 1925); 6: Rascaño (Guerrero Sala & Lorenzo Lizalde, 1981); 7: La Chora (González Echegaray, García Guinea, Begines Ramírez & Madariaga de la Campa, 1963); 8: Mirón (HS; Carretero et al., 2015); 9: Arrillor (N, Bermúdez de Castro & Sáenz de Buruaga, 1999); 10: Axlor (N; HS; this work); 11: Lezetxiki (N; Basabe, 1970); 12: Santa Catalina (HS; Albisu Andrade, Etxeberria Gabilondo, & Herrasti Erlogorri, 2014); 13: Aitzbitarte III (HS; de la Rúa & Hervella, 2011); 14: Alkerdi (Barandiarán & Cava, 2008); 15: Isturitz (HS; Henry-Gambier, Normand, & Pétilion, 2013); 16: Duruthy (HS; Henry-Gambier, 2006). N=Neandertal; HS=Homo sapiens. Base map made with QGIS 2.18.17 (QGIS Development Team, 2009) with data by Jarvis, Reuter, Nelson, & Guevara (2008).

180x120mm (600 x 600 DPI)

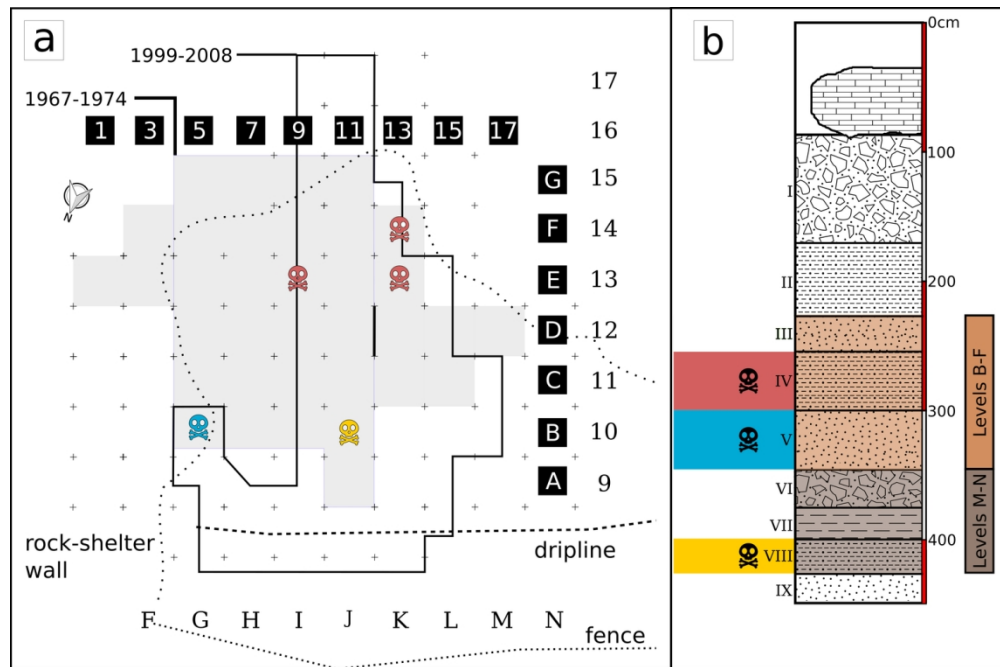
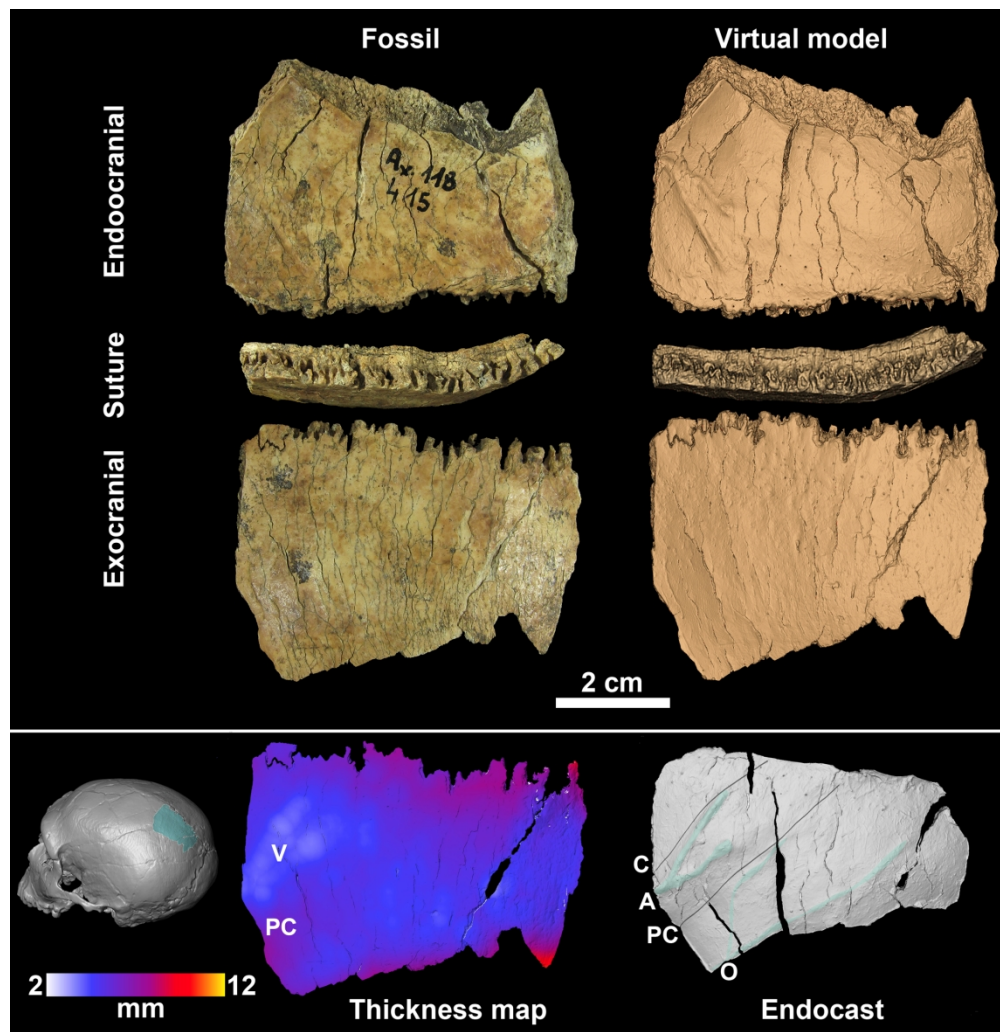


FIGURE 2 Excavation plan (a) and stratigraphic column (b) of Axlora cave (modified from Gómez-Olivencia et al., 2018a). (a) In the excavation plan the grid system used by J.M. Barandiarán (black square and white numbers) and the excavation area is shadowed in gray. The grid system used by the recent excavations is marked using black letters and numbers and the excavation area is outlined using a thick black line. The dotted line represents the rock-shelter wall when the site was first excavated, during the excavation this wall went back, revealing a possible cave infilling. The colors correspond to the levels to which these remains were attributed based on the notes by Barandiarán. (b) Synthetic section of the 1967–1974 excavation stratigraphy, drawn from the description of the layers by J. M. Barandiarán (1980). Different levels are marked with different colors, and the human remains are marked by silhouettes.

132x87mm (300 x 300 DPI)





39  
40  
41  
42  
43  
44  
45

FIGURE 3 Ax.11B.415.400 left parietal fragment. The original fossil and the 3D model are shown on different views. On the lower row, the approximate location of this fragment is shown on the La Ferrassie 1 Neanderthal cranium (left), a thickness map (from 2 to 12 mm) is shown (middle) with PC that correspond to thicker bone where is located the postcentral sulcus and V to a relative thinning produced by the anterior ramus of the meningeal system; and the anatomical features on the endocranial surface (right): including meningeal veins, A = anterior branch, O = obelic branch, and sulcal imprints C = central sulcus, PC = postcentral sulcus.

46  
47  
48  
49  
50  
51  
52  
53  
54  
55  
56  
57  
58  
59  
60

180x184mm (300 x 300 DPI)

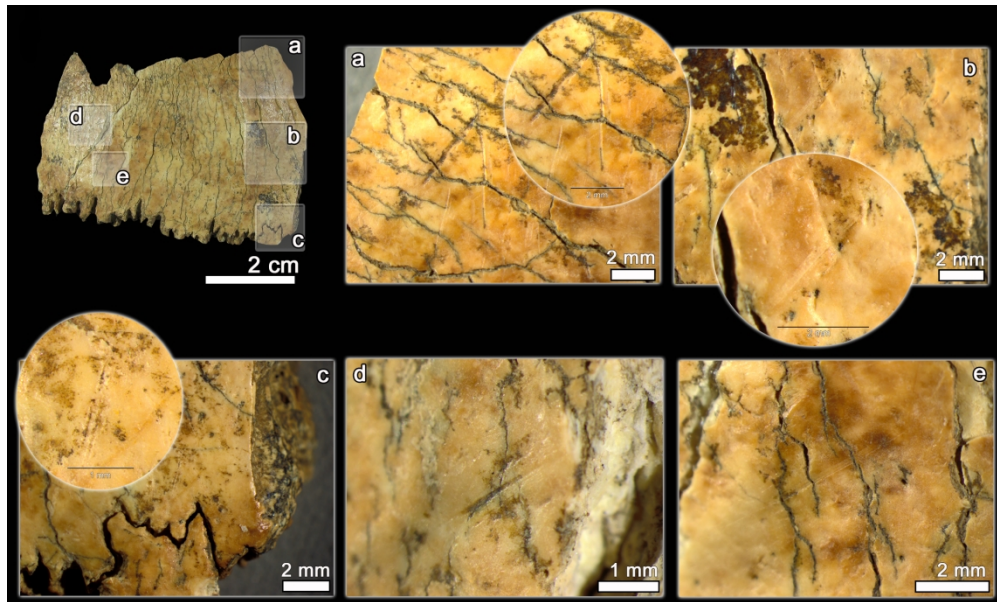


FIGURE 4 Ectocranial view of the specimen Ax.11B.415.400 with the location of zones a-d, and detailed images of these zones, where striations are located. In some cases, the grooves show a close "V" shape but do not show microstriations. The general morphology of these grooves (see text) make them compatible with trampling marks.

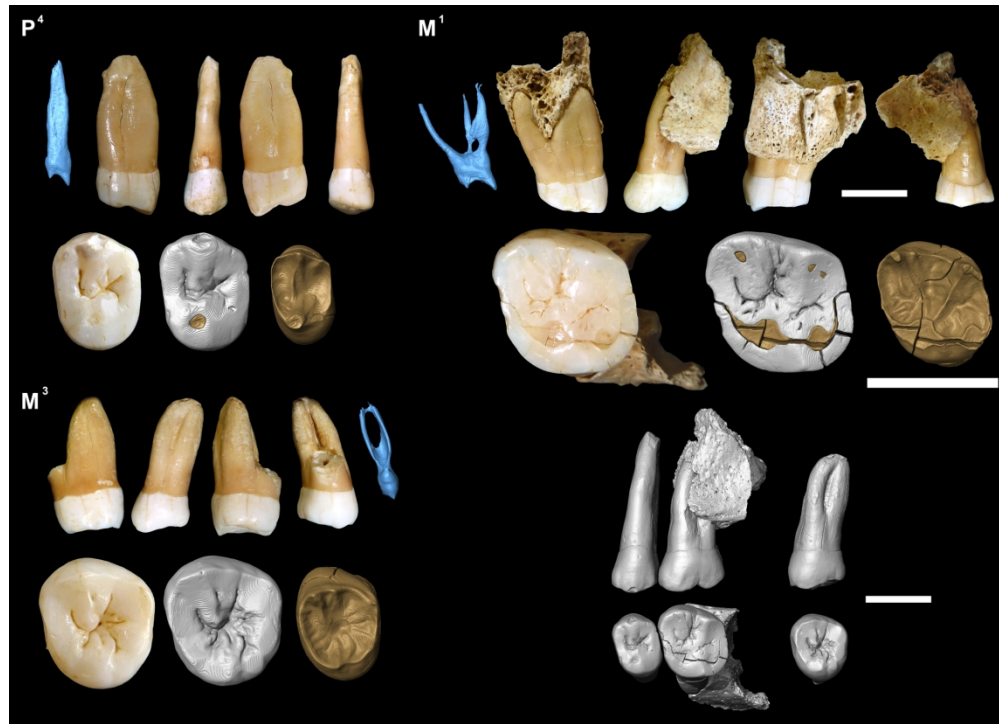
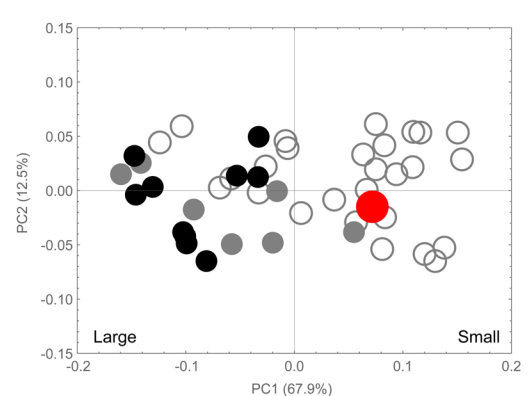
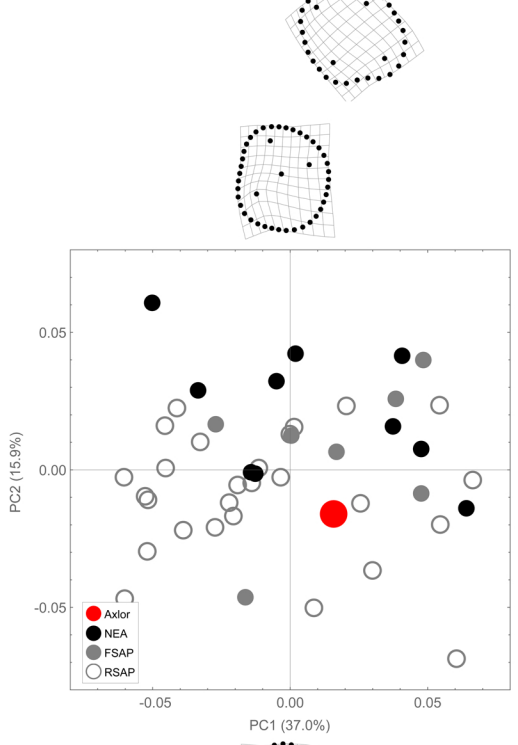
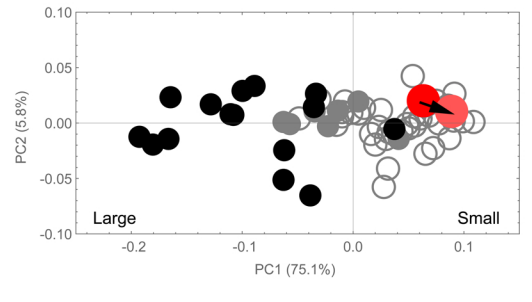
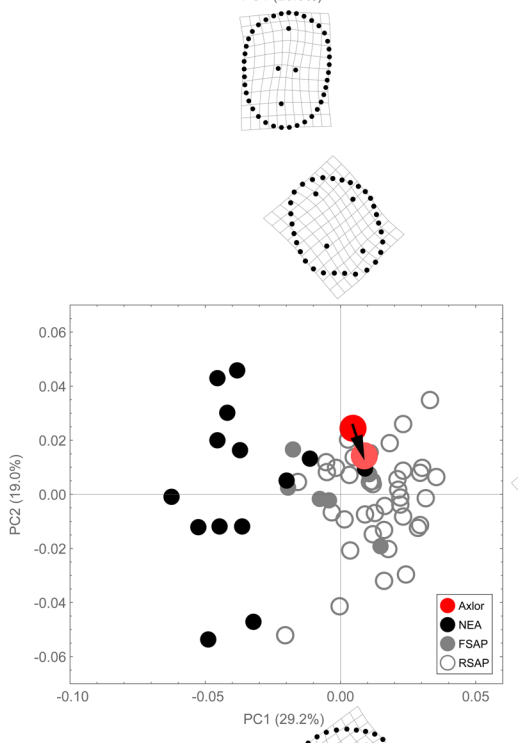
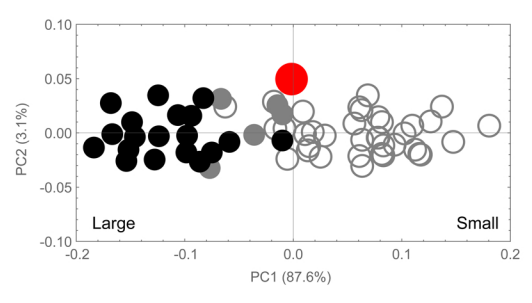
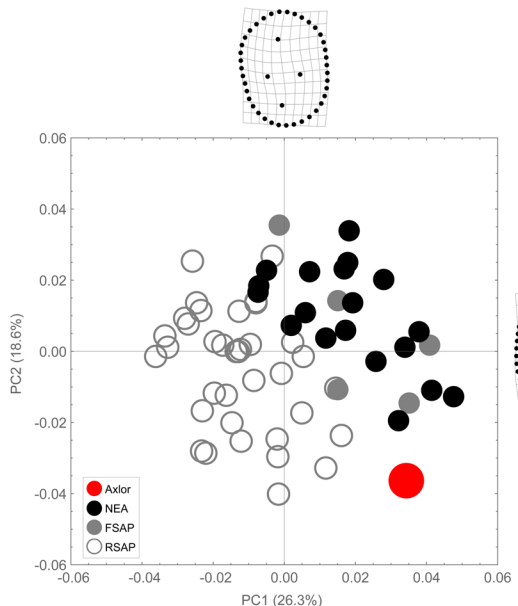


FIGURE 5 Dental remains previously studied by Basabe (1973) and Rostro-Carmona (2013), and likely belonging to the same individual. The teeth are shown in mesial, buccal, distal, lingual (top) and occlusal (bottom) views, together with the results of the enamel segmentation and the EDJ surface morphology. Pulp chamber volumes (in blue) are shown in mesial (P4, M1) and lingual (M2) views. A virtual reconstruction of the teeth in buccal and occlusal views is also provided. Scale bars = 1 cm.

180x129mm (300 x 300 DPI)

1 P<sup>4</sup>  
2  
3  
4  
5  
6  
7  
8  
9  
10  
11  
12  
13  
14  
15  
16  
17  
18  
19  
20  
21  
22  
23  
24  
25 M<sup>1</sup>  
26  
27  
28  
29  
30  
31  
32  
33  
34  
35  
36  
37  
38  
39  
40  
41  
42  
43  
44  
45  
46  
47 M<sup>3</sup>  
48  
49  
50  
51  
52  
53  
54  
55  
56  
57  
58  
59  
60



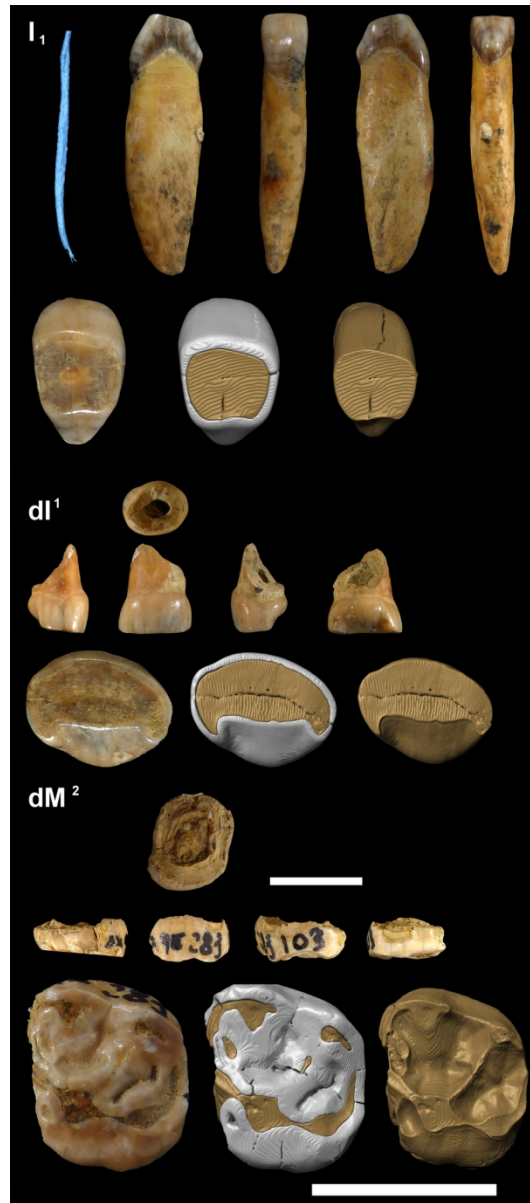


FIGURE 7 New dental remains from the Barandiarán collection of Axlór. AX.5B.299.16 (right permanent first lower incisor, I1): root canal morphology (blue) in mesial view; mesial, buccal, distal, lingual and occlusal views. AX.5B.299.31.64.17 (upper left first deciduous incisor, dI1): top, mesial, buccal, distal, lingual and occlusal views. AX.9E.283.103 (left dM2): top, mesial, buccal, distal, lingual and occlusal views. In the virtual reconstructions, enamel is represented in white and dentine in brown. Scale bars = 1 cm

80x180mm (300 x 300 DPI)